CHAPTER 3

Dynamics of Acoustic Bubbles

Kyuichi Yasui
National Institute of Advanced Industrial Science and Technology (AIST), Nagoya, Aichi, Japan

Chapter Outline

3.1 What is Acoustic Cavitation?

3.1.1 What is Cavitation?

A careful observer will be aware of the large number of bubbles generated around a ship's or motor boat's propeller when it is operating. Even when a ship's propeller is completely

Sonochemistry and the Acoustic Bubble. http://dx.doi.org/10.1016/B978-0-12-801530-8.00003-7

below the water's surface, such that air is not directly mixed with the water, a considerable number of bubbles are generated around the blades of the rotating propeller. This is due to the decrease in pressure near the surface of a propeller's blade that causes the creation of bubbles from gas nuclei on the blade itself and the gas dissolved in surrounding water. (See also Section 3.3.)

As the liquid pressure decreases near a rotating propeller's surface due to fluid flow, bubble nuclei in crevices on the surface of the propeller's blade expand. This causes gas in the surrounding liquid to enter the bubble according to Henry's law, and larger bubbles are formed.

The decrease in pressure is only at some specific regions near the rotating blades of a propeller, and the pressure recovers to the ambient one sufficiently distant from these regions [1]. When the generated bubbles move to the place where the liquid pressure is considerably higher, each bubble violently collapses (see Section 3.2.2). When a bubble violently collapses, a spherical shock wave is emitted from the bubble (see Section 3.4.3). Also, when a bubble violently collapses near a solid surface such as a propeller blade, a liquid jet penetrates the bubble and hits the solid surface (see Section 3.4.2). These types of events, occurring multiple times, eventually lead to the erosion of the propeller blades.

The generation of bubbles due to the decrease in liquid pressure and subsequent violent collapse of each bubble is a phenomenon known as cavitation [1–5]. When the decrease in liquid pressure is associated with the hydrodynamic motion of the liquid, such as the liquid flow around a spinning propeller, the associated cavitation is called hydrodynamic cavitation. Alternatively, when the decrease in liquid pressure is associated with the propagation of an intense acoustic (ultrasonic) wave, which is a wave of pressure oscillation, the associated cavitation is called acoustic cavitation. The bubbles generated in acoustic cavitation are called acoustic bubbles or acoustic cavitation bubbles.
A photograph of acoustic cavitation in water irradiated with 100 kHz ultrasound is shown in Figure 3.1.

3.1.2 Conditions for Cavitation to Occur

In hydrodynamic cavitation, many large bubbles are often generated that are visible to the naked eye, as in the case of cavitation at a ship's propeller. The condition required to generate such large bubbles is the decrease of liquid pressure below the saturated vapor pressure of the liquid [5]. It is a similar condition to that of boiling, with the difference being the violent collapse of many bubbles that occurs in cavitation.

In the case of acoustic cavitation, a drop in pressure on a liquid below the saturated vapor pressure of the liquid is often insufficient to generate bubbles. In most cases, the local liquid pressure needs to be decreased to a negative value for bubbles to be generated. This

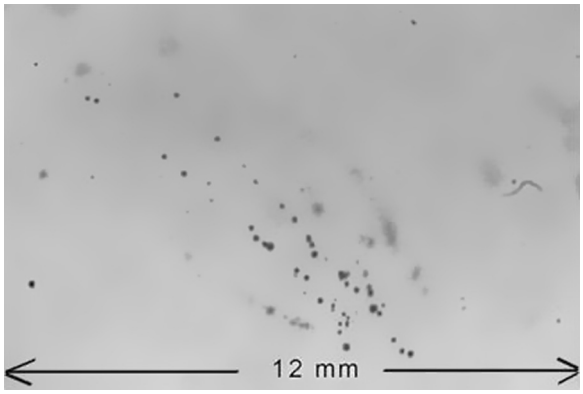

Figure 3.1
Bubbles in an acoustic cavitation field at 100 kHz.

is a consequence of the much shorter duration of low-pressure conditions associated with the passage of an acoustic wave compared with what the fluid experiences during the hydrodynamic motion of a liquid. During the compression phase of an acoustic wave after the rarefaction (low pressure) phase, small bubble nuclei essentially disappear.

What is meant by the negative pressure of a liquid? Negative pressure is only possible in a liquid or a solid; it is impossible to bring about in a gas. (However, it should be noted that negative pressure is occasionally defined in another way: pressure below atmospheric. In that case, negative pressure is possible also in a gas.) Consider the pressure in liquid water at 0 °C in a closed cylinder with a piston at the bottom connected to a hanging weight (Figure 3.2). When the mass of the weight is relatively small, the liquid pressure is still positive because the atmospheric pressure acts on the outer surface of the piston. However, when the mass of the weight is sufficiently large, the liquid senses a negative pressure.

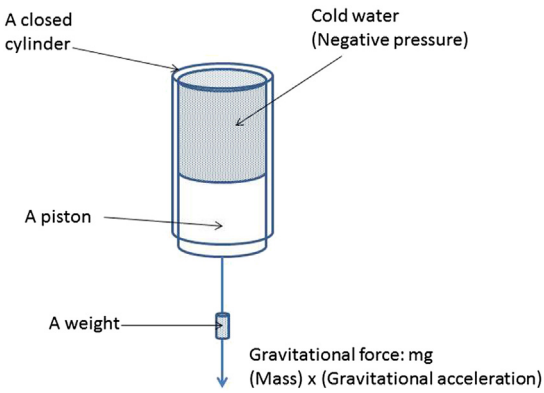

Figure 3.2
Negative pressure caused by pulling a piston in a closed cylinder filled with cold water.

(If the temperature of the liquid is higher than 0 °C, the liquid boils when the liquid pressure drops below the saturated vapor pressure.) The negative pressure is the tension acting to expand the liquid volume. In such a situation, many gas bubbles are generated, and the piston drops from the cylinder. The phenomenon is similar to acoustic cavitation in the sense that many gas bubbles are generated under a negative pressure.

Here, we again discuss acoustic cavitation. As the frequency of an acoustic wave (specifically an ultrasonic wave) increases, the duration of the rarefaction phase decreases because the period of pressure oscillation decreases. As a result, it becomes more difficult to generate bubbles. In other words, in order to achieve acoustic cavitation it is necessary to increase the pressure-amplitude of rarefaction (acoustic amplitude) as the ultrasonic frequency increases.

The minimum acoustic amplitude for cavitation to occur is called the cavitation threshold. In Figure 3.3, the cavitation threshold at an ultrasonic frequency of 26.3 kHz is shown as a function of the degree of saturation of air in water [6]. (Full saturation corresponds to 100%.) As the cavitation threshold strongly depends on the concentration of impurities in water as well as that of crevices on the wall of a liquid container, the experimental data shown in Figure 3.3 is only an example.

As seen in Figure 3.3, in degassed water the cavitation threshold is much higher than that in water saturated with gas (air). This indicates that gas dissolved in the liquid plays a major role in acoustic cavitation. In the next section, a theory accounting for the cavitation threshold is discussed.

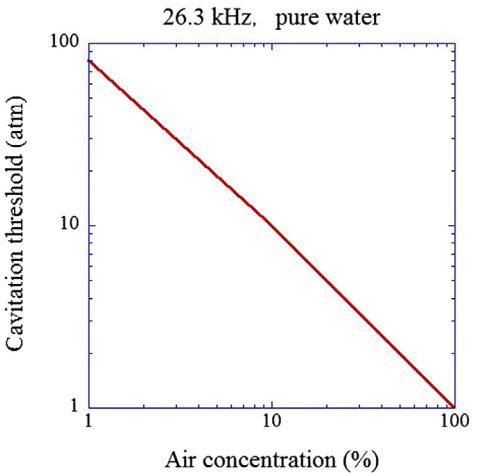

Figure 3.3
The cavitation threshold as a function of air concentration in pure water (degree of saturation) at an ultrasound frequency of 26.3 kHz.

3.1.3 The Condition for Large Expansion of a Bubble (Blake Threshold)

First, we will consider the relationship between the pressure inside and outside a bubble (Figure 3.4). The surface tension of the bubble–gas interface plays a major role in the pressure experienced inside a bubble [7]. Surface tension σ is the surface energy per unit area and is 7.275×10^{-2} [N/m] (=[J/m^2]) for pure water at 20 °C. When the bubble radius is R, the total surface energy of a bubble is $4\pi\sigma R^2$, as the surface area is $4\pi R^2$.

The work needed to expand a bubble by dR in radius (resulting in the surface area of $4\pi(R + dR)^2$) is $8\pi\sigma R dR$, neglecting the $(dR)^2$ term as dR is sufficiently small. As the work equals the force multiplied by the distance moved, the force equals $8\pi\sigma R$. Then, the balance between the force inside and outside a bubble is expressed by $4\pi R^2 p_{in} = 4\pi R^2 p_B + 8\pi\sigma R$, where p_{in} is the pressure inside a bubble and p_B is the liquid pressure outside a bubble. Finally, the following relationship is obtained:

$$p_{in} = p_B + \frac{2\sigma}{R} \tag{3.1}$$

The second term on the right side of Eqn (3.1) is called the Laplace pressure. A bubble's internal pressure is higher than the liquid pressure outside the bubble by the amount of the Laplace pressure.

A bubble's internal pressure is the sum of the gas (p_g) and vapor (p_v) pressures. Whereas the gas pressure dramatically changes according to the expansion and collapse of a bubble, the vapor pressure is assumed to remain constant at the saturated vapor pressure, even

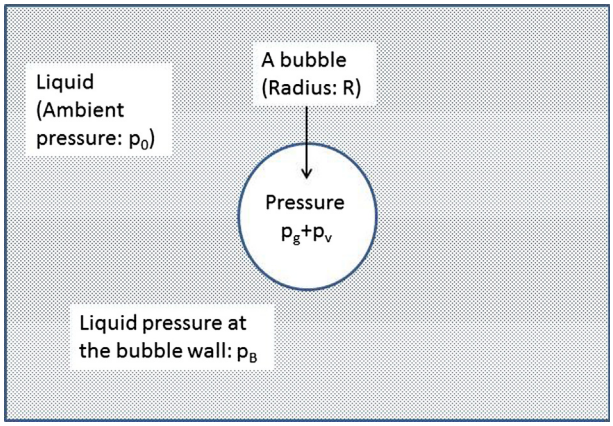

Figure 3.4
A diagrammatic representation of the relationship between the internal pressure of a bubble and the surrounding liquid pressure.

during the bubble's pulsation. The gas pressure inside a bubble is approximately expressed by Eqn (3.2):

$$p_g V^{\kappa} = const. \tag{3.2}$$

where V is the bubble volume and κ is a constant. When the heat transfer between a bubble and the surrounding liquid is negligible, the bubble pulsation becomes an adiabatic process resulting in $\kappa = \gamma = C_p/C_v$, where γ is called the specific-heat ratio, and C_p and C_v are the specific heats at constant pressure and constant volume, respectively. ($\gamma = 1.4$ for air.) When the bubble pulsation is mild, it becomes an isothermal process resulting in $\kappa = 1$. In reality, the bubble pulsation is neither adiabatic nor isothermal, resulting in the variation of κ between 1 and γ.

Here, a static bubble is considered in a liquid in the absence of ultrasound irradiation. The gas pressure inside a static bubble ($p_{g,s}$, where g and s denote gas and a static bubble, respectively) is expressed by Eqn (3.3) using Eqn (3.1) with $p_B = p_0 =$ the static ambient pressure, usually equivalent to 1 atm:

$$p_{g,s} = p_0 + \frac{2\sigma}{R_0} - p_v \tag{3.3}$$

where R_0 is the bubble radius in the absence of ultrasound (ambient (equilibrium) bubble radius), and the relationship $p_{in} = p_{g,s} + p_v$ is used.

Next, a bubble pulsates in a liquid irradiated by ultrasound, and the bubble radius temporally changes. When the instantaneous bubble radius is R, the gas pressure inside a bubble (p_g) is expressed by Eqn (3.4) using Eqn (3.2):

$$p_g = p_{g,s}\left(\frac{R_0}{R}\right)^{3\kappa} = \left(p_0 + \frac{2\sigma}{R_0} - p_v\right)\left(\frac{R_0}{R}\right)^{3\kappa} \tag{3.4}$$

using $V = 4\pi R^3/3$. Then, the liquid pressure at the bubble wall (p_B) is expressed by Eqn (3.5) using Eqn (3.1) and $p_{in} = p_g + p_v$:

$$p_B = \left(p_0 + \frac{2\sigma}{R_0} - p_v\right)\left(\frac{R_0}{R}\right)^{3\kappa} + p_v - \frac{2\sigma}{R} \tag{3.5}$$

The result of the numerical calculation of Eqn (3.5) is shown in Figure 3.5 for an air bubble with $R_0 = 10$ μm in pure water at 20 °C. The minimum value of p_B is −0.014 bar[1] at $R = 30$ μm. If the liquid pressure during the rarefaction phase of an ultrasound wave is lower than this value, the bubble will dramatically expand.

[1] 1 bar $= 10^5$ Pa $= 10^5$ N/$m^2 = 0.98692$ atm, 1 atm $= 1.01325 \times 10^5$ Pa.

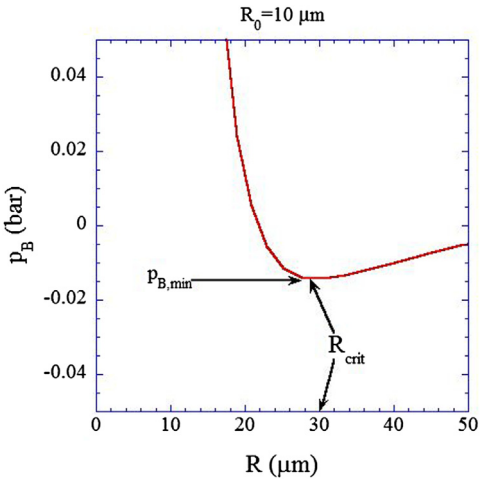

Figure 3.5

The liquid pressure at the bubble wall (p_B) as a function of the instantaneous bubble radius (R) when the ambient (equilibrium) bubble radius is $R_0 = 10$ μm (Eqn (3.5)).

Next, we will analytically calculate the minimum value of p_B in order to identify the acoustic amplitude required for a large expansion of a bubble. Firstly, p_B in Eqn (3.5) is differentiated with respect to R:

$$\frac{\partial p_B}{\partial R} = -3\kappa\left(p_0 + \frac{2\sigma}{R_0} - p_v\right)R_0^{3\kappa}R^{-(3\kappa+1)} + \frac{2\sigma}{R^2} \tag{3.6}$$

When p_B takes the minimum value, $\partial p_B/\partial R = 0$. If the value of R at this condition is expressed by R_{crit}, Eqn (3.6) yields Eqn (3.7):

$$(R_{crit})^{3\kappa-1} = \frac{3\kappa}{2\sigma}\left(p_0 + \frac{2\sigma}{R_0} - p_v\right)R_0^{3\kappa} \tag{3.7}$$

Here, we will consider a bubble expansion because the minimum value of p_B is always observed for a bubble radius larger than R_0 ($R_{crit} > R_0$). The expansion of a bubble in a liquid irradiated by ultrasound is a relatively slow process, because it involves the compression of the surrounding liquid. Thus, in most cases, bubble expansion is nearly an isothermal process. (The internal bubble temperature approximately equals the temperature of the liquid surrounding the bubble.) Then, $\kappa = 1$ is a good approximation:

$$R_{crit} = \sqrt{\frac{3R_0^3}{2\sigma}\left(p_0 + \frac{2\sigma}{R_0} - p_v\right)} \tag{3.8}$$

Finally, the minimum value of p_B ($p_{B,\min}$) is obtained by inserting Eqn (3.8) into Eqn (3.5):

$$p_{B,\min} = p_v - \frac{4\sigma}{3}\sqrt{\frac{2\sigma}{3R_0^3\left(p_0 + \frac{2\sigma}{R_0} - p_v\right)}} \tag{3.9}$$

When a liquid is irradiated by ultrasound, the liquid pressure far from a bubble is expressed by $p_0 + p_S(t)$, where p_0 is the static ambient pressure and $p_S(t)$ is the instantaneous pressure of the ultrasound wave at time t. If this pressure is lower than the liquid pressure at the bubble wall (p_B), then the bubble will expand. If the pressure is even lower than the minimum value of p_B given by Eqn (3.9), then the bubble will continue to expand indefinitely. When the pressure-amplitude of ultrasound (acoustic amplitude) and its angular frequency are expressed by A and ω, respectively, then $p_S(t) = A\sin\,\omega t$, and the minimum value of $p_S(t)$ is -A. Thus, if p_0-A is smaller than the minimum value of p_B in Eqn (3.9), a bubble will dramatically expand. The threshold condition is given by Eqn (3.10):

$$A_{Blake} = p_0 - p_{B,\min} = p_0 - p_v + \frac{4\sigma}{3}\sqrt{\frac{2\sigma}{3R_0^3\left(p_0 + \frac{2\sigma}{R_0} - p_v\right)}} \tag{3.10}$$

The condition for a bubble to dramatically expand is $A \geq A_{Blake}$, where A_{Blake} is called the Blake threshold.

In Figure 3.6, the Blake threshold is shown as a function of the ambient bubble radius (R_0) according to Eqn (3.10). When the ambient radius is larger than 1 μm, the Blake threshold nearly equals 1 atm (the static ambient pressure). When the radius is smaller than 1 μm, an

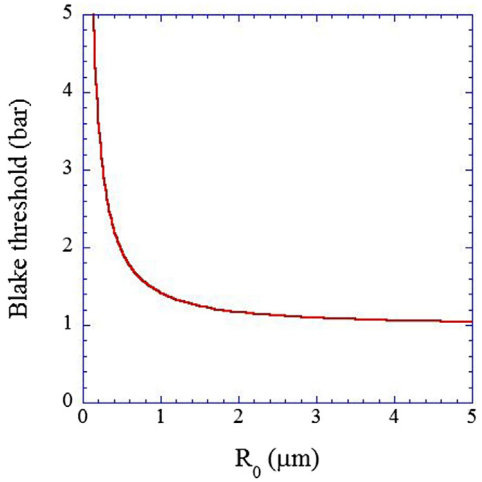

Figure 3.6
The Blake threshold as a function of the ambient (equilibrium) bubble radius (Eqn (3.10)).

acoustic amplitude much greater than 1 atm is required for a bubble to dramatically expand. The validity of Eqn (3.10) is limited, however, to the case of relatively low ultrasonic frequencies (less than about 20 kHz), and much higher acoustic amplitudes are required at higher ultrasonic frequencies due to the shorter duration of the rarefaction phase. It remains a problem to be solved in the future, where the effect of ultrasonic frequency is taken into account in Eqn (3.10).

As will be discussed in the following sections, it is often the case that a bubble will violently collapse after a large radial expansion. Thus, the Blake threshold is often referred to as the cavitation threshold.

3.2 Bubble Dynamics

3.2.1 The Rayleigh–Plesset Equation

Here, the Rayleigh–Plesset equation for bubble pulsation is more intuitively derived than in Chapter 2 [2,4]. A liquid volume with radius R_L surrounding a bubble is considered—it is much larger than the bubble radius but much smaller than a particular wavelength of ultrasound (Figure 3.7). When a bubble is pulsating, the liquid volume also pulsates and has some kinetic energy. The kinetic energy (E_K) of the liquid volume is estimated as follows. The spherical shell of liquid with thickness dr and radius r from the center of a spherical bubble has kinetic energy of $1/2 \times 4\pi r^2 \rho dr$ (the mass) $\times \dot{r}^2$ (square of velocity), where ρ is the liquid density and the dot denotes the time derivative (d/dt). The total kinetic energy (E_K) of the liquid volume is the integration of the above quantity with respect to r from R to R_L, where R is the instantaneous bubble radius:

$$E_K = \frac{1}{2}\rho \int_R^{R_L} \dot{r}^2 4\pi r^2 dr = 2\pi\rho R^3 \dot{R}^2 \tag{3.11}$$

where incompressibility of the liquid ($4\pi r^2 \dot{r} = 4\pi R^2 \dot{R}$) as well as $R << R_L$ are assumed.

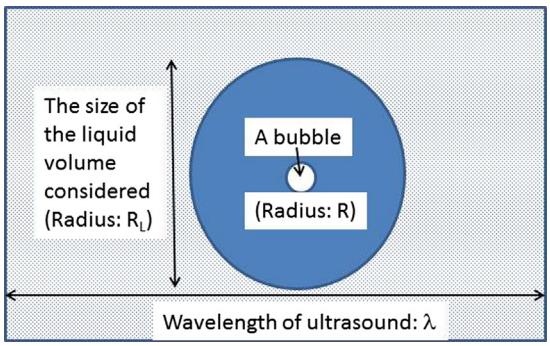

Figure 3.7
Derivation of the Rayleigh–Plesset equation of bubble pulsation.

When a bubble expands, it does work on the surrounding liquid. On the other hand, when a bubble collapses, the surrounding liquid does work on the bubble. In other words, the bubble does negative work on the surrounding liquid. The work (W_{bubble}) that a bubble does on the surrounding liquid from the initial state, with ambient bubble radius (R_0), to the state at time t with instantaneous bubble radius (R), is given by Eqn (3.12):

$$W_{bubble} = \int_{R_0}^{R} 4\pi r^2 p_B dr \tag{3.12}$$

where p_B is the liquid pressure at the bubble wall.

When a bubble expands, the liquid volume of initial radius R_L moves slightly outward. In other words, the liquid volume does work on the surroundings. When a bubble collapses, the liquid volume moves slightly inward. In other words, work is done on the liquid volume by the surroundings. (The liquid volume does negative work.) The work (W_{liquid}) done by the liquid volume of initial radius of R_L is given by Eqn (3.13):

$$W_{liquid} = p_\infty \Delta V = p_\infty \int_{R_0}^{R} 4\pi r^2 dr \tag{3.13}$$

where p_∞ is the pressure at the surface of the liquid volume (ambient static pressure + instantaneous acoustic pressure), and ΔV is the volume swept out by the liquid outside the radius of R_L when a bubble expands (when a bubble collapses, $\Delta V < 0$). In the last Eqn (3.13), incompressibility of the liquid is assumed (the total volume of the liquid is assumed to be constant).

The energy conservation law yields the following relationship:

$$W_{bubble} = E_K + W_{liquid} \tag{3.14}$$

Differentiation of Eqn (3.14) with respect to R yields Eqn (3.15), using the relationship Eqn (3.16):

$$\frac{p_B - p_\infty}{\rho} = \frac{3\dot{R}^2}{2} + R\ddot{R} \tag{3.15}$$

$$\frac{\partial\left(\dot{R}^2\right)}{\partial R} = \frac{1}{\dot{R}} \frac{\partial\left(\dot{R}^2\right)}{\partial t} = 2\ddot{R} \tag{3.16}$$

When a bubble pulsates, the effect of the liquid viscosity is not negligible, and should be taken into account in the calculation of p_B. The pressure at the bubble wall due to

viscosity is given by $2\mu\frac{\partial\dot{r}}{\partial r}|_{r=R}$, where μ is liquid viscosity and $\dot{r} = dr/dt$ is liquid velocity [2]. Then, Eqn (3.1) is modified as Eqn (3.17):

$$p_B = p_g + p_v - \frac{2\sigma}{R} + 2\mu\frac{\partial\dot{r}}{\partial r}\bigg|_{r=R} = p_g + p_v - \frac{2\sigma}{R} - \frac{4\mu\dot{R}}{R} \tag{3.17}$$

where p_g and p_v are the partial pressures of the permanent gas and the vapor pressure inside a bubble, respectively. In the last part of Eqn (3.17), the incompressibility of the liquid is assumed ($4\pi r^2\dot{r} = 4\pi R^2\dot{R}$).

Inserting Eqn (3.17) into Eqn (3.15) yields the Rayleigh–Plesset equation:

$$R\ddot{R} + \frac{3\dot{R}^2}{2} = \frac{1}{\rho}\left(p_g + p_v - \frac{2\sigma}{R} - \frac{4\mu\dot{R}}{R} - p_0 - p_s(t)\right) \tag{3.18}$$

where p_0 is the ambient static pressure and $p_s(t)$ is the instantaneous acoustic pressure at time t ($p_\infty = p_0 + p_s(t)$). As liquid incompressibility has been assumed in the derivation (Eqns (3.11), (3.13), and (3.17)), Eqn (3.18) is no longer valid when a bubble strongly collapses, and the magnitude of the bubble wall velocity $\dot{R}$ becomes comparable to the sound speed in the liquid.

There are several equations that account for liquid compressibility to the first order of $\dot{R}/c_\infty$, where c_∞ is the speed of sound in the liquid far from a bubble (about 1500 m/s in pure water) [8]:

$$\begin{aligned}\left(1 - (\Lambda+1)\frac{\dot{R}}{c_\infty}\right)R\ddot{R} + \frac{3\dot{R}^2}{2}\left(1 - \frac{1}{3}(3\Lambda+1)\frac{\dot{R}}{c_\infty}\right)\\ = \frac{1}{\rho}\left(1 + (1-\Lambda)\frac{\dot{R}}{c_\infty}\right)\left[p_B - p_S\left(t + \frac{R}{c_\infty}\right) - p_0\right] + \frac{R}{c_\infty\rho}\frac{dp_B}{dt}\end{aligned} \tag{3.19}$$

where $p_S\left(t + \frac{R}{c_\infty}\right)$ is the instantaneous acoustic pressure at time $t + R/c_\infty$, and Λ is an arbitrary constant smaller than $c_\infty/|\dot{R}|$ in magnitude. Equation (3.19) with $\Lambda = 0$ and $\Lambda = 1$ are referred to as the Keller and Herring equations, respectively. The Keller equation seems to agree well with the experimental data of the bubble radius as a function of time. However, Eqn (3.19) is valid only when $\dot{R}/c_\infty$ is smaller than 1 in magnitude, and an equation valid for larger magnitude of $\dot{R}/c_\infty$ than 1 is unknown at present. The derivation (or discovery) of such an equation is a future task. Of relevance, there have been a few studies based on direct numerical simulations of bubble collapse employing fundamental equations of fluid dynamics [9,10].

3.2.2 The Rayleigh Collapse

Here, a bubble collapse is discussed using Rayleigh–Plesset Eqn (3.18). The bubble wall acceleration ($\ddot{R}$) is expressed as follows using Eqn (3.18):

$$\ddot{R} = -\frac{3\dot{R}^2}{2R} + \frac{1}{\rho R}\left(p_g + p_v - \frac{2\sigma}{R} - \frac{4\mu\dot{R}}{R} - p_0 - p_S(t)\right) \tag{3.20}$$

When a bubble violently collapses and $\dot{R}^2$ increases, the first term on the right side of Eqn (3.20) becomes dominant, and the second term is negligible:

$$\ddot{R} \approx -\frac{3\dot{R}^2}{2R} \tag{3.21}$$

This means that the bubble wall acceleration ($\ddot{R}$) is always negative. Negative acceleration means that the bubble wall velocity ($\dot{R}$) decreases. During the bubble collapse ($\dot{R} < 0$), the magnitude of the velocity increases, and the magnitude of the right side of Eqn (3.21) increases. Accordingly, the magnitude of the bubble wall acceleration ($\ddot{R} < 0$) increases, and the magnitude of the bubble wall velocity further increases, in a self-sustaining process. Such an autonomously accelerating collapse of a bubble is known as a Rayleigh collapse.

Question 3.1

What is the physical reason for the freely accelerating collapse of a bubble?

Answer 3.1

Two spherical surfaces of the liquid surrounding a collapsing bubble are considered as in Figure 3.8. The radii of the spheres are R_1 and R_2 ($R_1 > R_2$). The liquid flows inwardly as a bubble collapses. The amount of liquid passing the spherical surface of radius R_1 per unit of

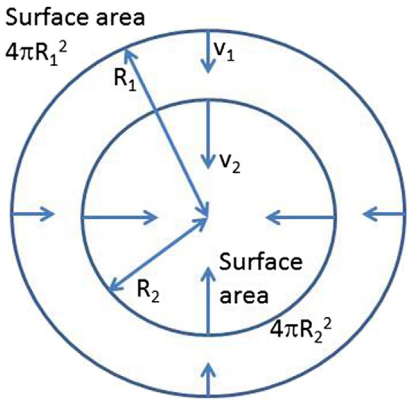

Figure 3.8
Spherically inward flow as the mechanism for the violent collapse of a bubble.

time is $4\pi R_1^2 v_1$, where v_1 is the liquid velocity at R_1. Similarly, that passing the spherical surface of radius R_2 is $4\pi R_2^2 v_2$. If the liquid is incompressible, the above amounts of liquid are equal. Then, $v_2 = v_1(R_1/R_2)^2 > v_1$. Thus, the spherically inward flow accelerates. This suggests that the bubble collapse freely accelerates.

Question 3.2

What is the time period of the Rayleigh collapse of a bubble?

Answer 3.2

The Rayleigh collapse starting from the maximum bubble radius ($R_{\max}$) is considered [1,11]. The work (W_{liquid}) done by the liquid volume of initial radius R_L given by Eqn (3.13) is expressed using $R_{\max}$ in this case as follows:

$$W_{liquid} = p_\infty \int_{R_{\max}}^{R} 4\pi r^2 dr = \frac{4}{3}\pi p_\infty \left(R^3 - R_{\max}^3\right) \tag{3.22}$$

Neglecting W_{bubble} in Eqn (3.12), as p_B is much smaller than p_∞ during the initial stage of bubble collapse, the energy conservation law (Eqn (3.14)) yields the following relationship:

$$\dot{R}^2 = \frac{2p_\infty}{3\rho}\left(\frac{R_{\max}^3}{R^3} - 1\right) \tag{3.23}$$

Then, the time of the bubble collapse ($t_{collapse}$) is given by the following equation:

$$t_{collapse} = \int_{R_{\max}}^{R=0} \frac{dR}{\dot{R}} = \sqrt{\frac{3\rho}{2p_\infty}} \int_{R_{\max}}^{R=0} \frac{-R^{3/2} dR}{\sqrt{R_{\max}^3 - R^3}} = R_{\max}\sqrt{\frac{3\rho}{2p_\infty}} \int_0^1 \frac{\beta^{3/2} d\beta}{\sqrt{1-\beta^3}} \tag{3.24}$$

where $\beta = R/R_{\max}$. The integral is expressed by means of Γ functions as follows:

$$\int_0^1 \frac{\beta^{3/2} d\beta}{\sqrt{1-\beta^3}} = \frac{1}{3}\int_0^1 z^{-1/6}(1-z)^{-1/2} dz = \frac{1}{3}\frac{\Gamma(5/6)\Gamma(1/2)}{\Gamma(4/3)} \sim 0.75 \tag{3.25}$$

where the following formula for the beta function (B(x,y)) is used [12]:

$$\mathrm{B}(x,y) = \int_0^1 t^{x-1}(1-t)^{y-1} dt = \frac{\Gamma(x)\Gamma(y)}{\Gamma(x+y)} \tag{3.26}$$

Finally, the time of the collapse is given as follows:

$$t_{collapse} \sim 0.9 R_{\max}\sqrt{\frac{\rho}{p_\infty}} \tag{3.27}$$

For example, when a bubble of maximum radius 100 μm collapses in water of density 10^3 kg/m^3 with $p_\infty = 1$ atm $= 1.01325 \times 10^5$ Pa, $t_{collapse} \sim$ 9 μs.

What happens at the final stage of a Rayleigh collapse? Inside a bubble in water, permanent gas (air, argon, etc.) and vapor (water) molecules are present. As the pressure inside a bubble increases during the collapse of the bubble, gas gradually dissolves into the surrounding liquid and vapor condenses at the bubble wall. Nevertheless, as the bubble wall speed is very high, appreciable amounts of gas and vapor remain inside the bubble. Consequently, the pressure inside the bubble further increases. In addition, the energy loss of a bubble by thermal conduction from the heated interior of the bubble to the surrounding liquid is much less than the energy gain of the bubble from the pV work of the surrounding liquid, due to the high speed of the bubble collapse. This makes bubble collapse a quasiadiabatic process, where "quasi" means that there is considerable thermal conduction between a bubble and the surrounding liquid. As a result, the temperature and the pressure inside a bubble dramatically increase during the collapse. Finally, the density inside a bubble reaches that of a condensed phase (liquid or solid) and gas pressure (p_g) increases to 100−1000 atm pressure. Then, the second term on the right side of Eqn (3.20) becomes larger than the first term, and the bubble wall acceleration ($\ddot{R}$) becomes positive. This stops bubble collapse, because the bubble wall velocity decreases in magnitude. At this moment, the temperature inside a bubble is more than a few thousands degrees Kelvin [4].

3.2.3 Numerical Simulation of Bubble Pulsation

For quantitative discussions on bubble pulsation, numerical simulations of the Rayleigh−Plesset Eqn (3.18), the Keller equation, or the Herring Eqn (3.19) are required.

The simplest method of numerical simulation is the Euler method [13−15]:

$$R(t+\Delta t) = R(t) + \dot{R}(t)\Delta t \tag{3.28}$$

In numerical calculations, the continuum time is divided into a large number of discrete times with a small unit step (Δt). The bubble radius at time $t + \Delta t$ is derived by the bubble radius and the bubble wall velocity at time t using the relationship Eqn (3.28). For the numerical calculations, the initial condition (R and $\dot{R}$ at $t = 0$) is required. The proof for Eqn (3.28) is the definition of the time derivative:

$$\dot{R}(t) = \lim_{\Delta t \to 0} \frac{R(t+\Delta t) - R(t)}{\Delta t} \tag{3.29}$$

In the calculation of the next step, the bubble wall velocity ($\dot{R}$) at $t + \Delta t$ is required:

$$R(t+2\Delta t) = R(t+\Delta t) + \dot{R}(t+\Delta t)\Delta t \tag{3.30}$$

The bubble wall velocity at $t + \Delta t$ is calculated using an equation similar to Eqn (3.28):

$$\dot{R}(t+\Delta t) = \dot{R}(t) + \ddot{R}(t)\Delta t \tag{3.31}$$

where the bubble wall acceleration $\ddot{R} = d^2R/dt^2$ is calculated by Eqn (3.20) for the Rayleigh–Plesset equation or by Eqn (3.19) for the Keller or Herring equation. Iteration of the calculation yields the radius–time curve. The time step (Δt) should be small enough such that the calculated result is independent of the value of Δt.

Results of the numerical simulations of the Keller equation are shown in Figures 3.9 and 3.10. The simulation is under the condition of single-bubble sonoluminescence (SBSL). SBSL is the light-emission phenomenon from a single stable bubble trapped at the pressure antinode of a standing acoustic wave in pure water (see Chapter 4). A bubble expands during the rarefaction phase of an ultrasound wave and collapses during the onset of the compression phase (Figure 3.9(a)). During the compression phase of an ultrasound wave, a bouncing motion of bubble pulsation is observed. In the following rarefaction phase of ultrasound, the bubble expands again. The process is repeated in a clocklike manner. During bubble expansion, water evaporates into a bubble at the bubble wall (Figure 3.9(b)). During bubble collapse, water vapor condenses at the bubble wall.

At the final stage of bubble collapse, the temperature inside a bubble increases to as much as 18,000 K, and light is emitted (Figure 3.10(a)). Due to the high temperature, water vapor is dissociated inside the bubble, and hydrogen (H_2), oxygen (O_2), and hydroxyl radicals (OH) are created (Figure 3.10(b)). OH plays an important role in chemical reactions associated with ultrasound (sonochemical reactions). Numerical simulations have suggested that an appreciable number of oxygen atoms (O) are created inside a bubble in addition to OH [16]. However, the lifetime of O atoms in the liquid phase (or at the bubble wall) is unknown at present. (The lifetime of OH in the liquid phase depends on its

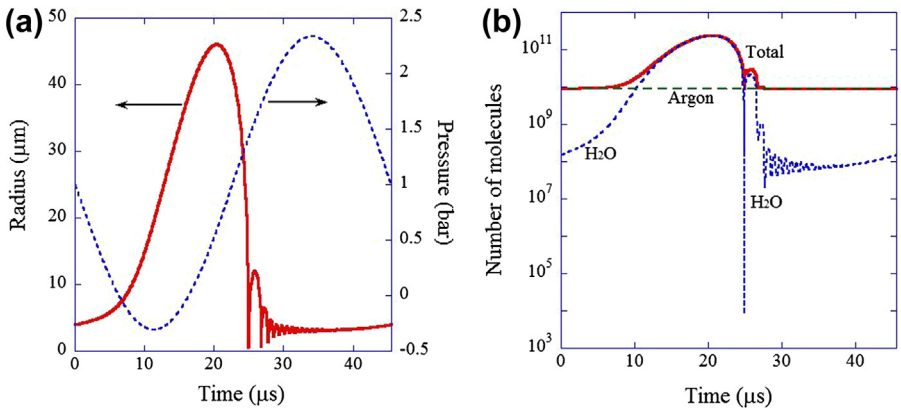

Figure 3.9

The results of numerical simulations of bubble pulsation as a function of time for one acoustic cycle. The frequency and pressure-amplitude of the acting ultrasound is 22 kHz and 1.32 bar, respectively. The ambient (equilibrium) bubble radius is 4 μm for an argon bubble in 20 °C water. (a) The bubble radius (solid line) and the pressure ($p_\infty = p_0 + p_S(t)$) (dotted line) (b) The number of molecules inside a bubble on a logarithmic scale.

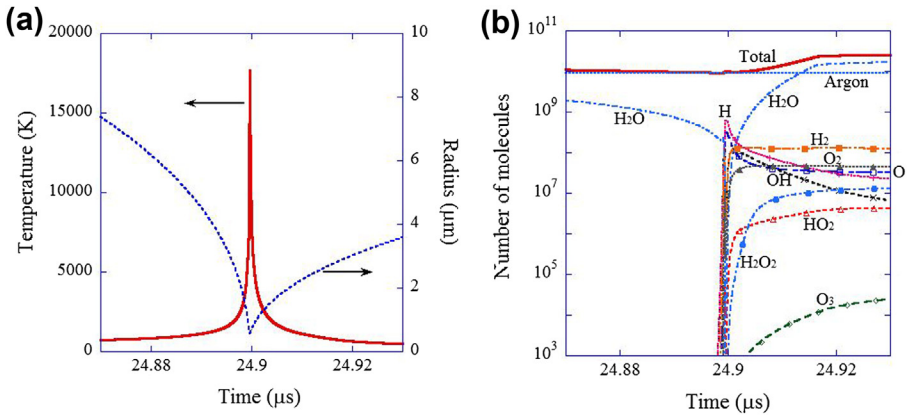

Figure 3.10

The results of numerical simulations around bubble collapse as a function of time, specifically for 0.06 μs (this condition is the same as that of Figure 3.9). (a) The bubble radius (dotted line) and the temperature inside a bubble (solid line). (b) The number of molecules inside a bubble on a logarithmic scale. At $t = 24.93$ μs (the right end of the graph), the main chemical products are H_2 (1×10^8 in number of molecules), O_2 (4×10^7), O (3×10^7), H (2×10^7), H_2O_2 (1×10^7), and OH (7×10^6).

concentration as well as the concentration of any reactive solute present in solution. Typically, the lifetime ranges from 10^{-7} to 10^{-4} s.)

In the numerical simulations of Figures 3.9 and 3.10, the permanent gas inside a bubble is assumed to be argon. Nitrogen, which is 78% of the composition of air, in mole fraction, is repeatedly burned inside an air bubble, and the resultant NOx and HNOx gradually dissolve into the surrounding liquid water. Inside a bubble, only chemically inactive argon, which constitutes 1% of air, remains. This is called argon rectification and has been confirmed both experimentally and theoretically [17].

Next, the calculation of the temperature inside a bubble is discussed. The temperature (T) is related to the internal thermal energy (E) of a bubble as follows:

$$E = nC_vT \tag{3.32}$$

where n is the number of gas and vapor molecules inside a bubble in mole, and C_v is the molar heat of gas and vapor at constant volume. The thermal energy (E) changes with time, associated with the expansion and collapse of a bubble:

$$\Delta E = -p\Delta V + 4\pi R^2 \kappa_T \left.\frac{\partial T}{\partial r}\right|_{r=R} \Delta t + \Delta H \tag{3.33}$$

where ΔE is the change in the internal thermal energy of a bubble, p is the pressure inside a bubble, ΔV is the volume change of a bubble, κ_T is the thermal conductivity of

gas and vapor, $\partial T/\partial r|_{r=R}$ is the temperature gradient at the bubble wall, Δt is the time step in the numerical calculation, and ΔH is the heat of chemical reaction inside a bubble. From the thermal energy of a bubble calculated using Eqn (3.33) during the bubble pulsation, the instantaneous temperature inside a bubble is estimated using Eqn (3.32). It should be noted that the number n of gas and vapor molecules inside a bubble in Eqn (3.32) dramatically changes with evaporation and condensation of water vapor at the bubble wall.

In general, during bubble expansion, the temperature inside a bubble nearly equals the ambient temperature due to the thermal conduction between a bubble and the surrounding liquid (an isothermal process) [18]. On the other hand, during bubble collapse, the temperature inside a bubble dramatically increases by the pV work of the surrounding liquid (a quasiadiabatic process). At the final stage of the collapse, however, the endothermic heat of chemical reactions considerably reduces the bubble temperature. As a result, the maximum temperature attained inside a bubble in water at the collapse is usually less than 30,000 K [19,20].

Question 3.3

Estimate the maximum temperature and pressure inside a bubble at the collapse if the bubble collapse is adiabatic (without any heat exchange between the interior of a bubble and the surrounding liquid).

Answer 3.3

The bubble collapse starting from the maximum bubble radius ($R_{\max}$) is considered [2]. The initial pressure inside a bubble is denoted by P_m. Then, the pressure (p_g) inside a bubble at radius R is given as follows by the adiabatic relationship of $pV^{\gamma} = \text{constant}$, where p is the pressure, V is the volume, γ is the specific-heat ratio ($\gamma = C_p/C_v$), and $C_p(C_v)$ is the molar heat at constant pressure (volume):

$$p_g = p_m \left(\frac{R_{\max}}{R}\right)^{3\gamma} \tag{3.34}$$

Then, the work that a bubble does on the surrounding liquid in Eqn (3.12) is approximately estimated by the following:

$$W_{bubble} = \int_{R_{\max}}^{R} 4\pi r^2 p_B dr \sim \frac{1}{1-\gamma}\frac{4\pi R_{\max}^3}{3} p_m \left(\left(\frac{R_{\max}}{R}\right)^{3(\gamma-1)} - 1\right) \tag{3.35}$$

where p_B is assumed to be nearly equal to p_g, and W_{bubble} is negative. Then, the energy conservation law (Eqn (3.14)) yields the following relationship:

$$\frac{3\rho\dot{R}^2}{2} \sim p_\infty \left(\left(\frac{R_{\max}}{R}\right)^3 - 1\right) + p_m \frac{1}{1-\gamma}\left(\left(\frac{R_{\max}}{R}\right)^{3\gamma} - \left(\frac{R_{\max}}{R}\right)^3\right) \tag{3.36}$$

At the end of the bubble collapse, the bubble wall velocity is 0 $\left(\frac{dR}{dt} = \dot{R} = 0\right)$ and the bubble radius takes the minimum value ($R_{\min}$). From Eqn (3.36), the following relationship holds, assuming ($R_{\max}/R_{\min}$) >> 1:

$$p_m \left(\frac{R_{\max}}{R_{\min}}\right)^{3(\gamma-1)} \sim p_\infty (\gamma - 1) \tag{3.37}$$

As the pressure inside a bubble at the minimum radius takes on the maximum value ($p_{g,\max}$), Eqns (3.34) and (3.37) yield the following relationship:

$$p_{g,\max} = p_m \left(\frac{R_{\max}}{R_{\min}}\right)^{3\gamma} \sim p_m \left(\frac{p_\infty (\gamma - 1)}{p_m}\right)^{\frac{\gamma}{\gamma-1}} \tag{3.38}$$

In the adiabatic process, $TV^{\gamma-1}$ = constant, where T is the temperature and V is the volume. The maximum temperature ($T_{\max}$) is at the minimum radius of a bubble in this case:

$$\frac{T_{\max}}{T_m} = \left(\frac{R_{\max}}{R_{\min}}\right)^{3(\gamma-1)} \tag{3.39}$$

where T_m is the initial temperature inside a bubble at $R_{\max}$. From Eqn (3.37), the following relationship holds:

$$T_{\max} \sim \left(\frac{p_\infty (\gamma - 1)}{p_m}\right) T_m \tag{3.40}$$

Now, Eqns (3.38) and (3.40) are applied for the condition of Figures 3.9 and 3.10. If we assume that the bubble expansion is isothermal at 293 K as pV = constant, p_m is estimated as follows using $R_0 = 4$ μm and $R_{\max} = 46$ μm:

$$p_m \sim p_\infty \left(\frac{R_0}{R_{\max}}\right)^3 \sim 70 \text{ Pa} \tag{3.41}$$

For argon, $\gamma = 5/3 \sim 1.67$ (For air, $\gamma \sim 1.4$). Thus, for an argon bubble, Eqns (3.38) and (3.40) yield $p_{g,\max} \sim 2 \times 10^9$ Pa and $T_{\max} \sim 280{,}000$ K. The values differ considerably from the result of the numerical simulation in Figures 3.9 and 3.10: $p_{g,\max} \sim 6 \times 10^9$ Pa and $T_{\max} \sim 18{,}000$ K. Thus, Eqns (3.38) and (3.40) do not work under actual situations. (With $p_m \sim 2.3 \times 10^3$ Pa, which is the saturated vapor pressure at 293 K, Eqns (3.38) and (3.40) yield $p_{g,\max} \sim 1 \times 10^7$ Pa and $T_{\max} \sim 8500$ K, which are again quite different from the results of the numerical simulation.) The reason for the failure of Eqns (3.38) and (3.40) is due to the neglect of thermal conduction between the heated interior of a bubble and the surrounding liquid, and that of nonequilibrium evaporation and condensation of water vapor at the bubble wall, as well as the thermal dissociation of water vapor inside a bubble.

3.2.4 Shock Wave Formation Inside a Collapsing Bubble

In the above discussions, the spatial homogeneity of pressure and temperature inside a bubble is assumed. However, under some conditions the bubble interior becomes strongly

inhomogeneous, such as in the case of shock wave formation. Under many of the conditions of SBSL, numerical simulations using fundamental equations of fluid dynamics (equations of continuity, momentum, and energy) have indicated that the temperature and pressure inside a bubble are nearly spatially uniform, except near the bubble wall [21]. Also, according to some numerical simulations, under certain conditions a spherically converging shock wave is formed inside a collapsing bubble. The conditions for shock formation inside a bubble need to be studied further, both experimentally and theoretically.

Question 3.4

Why is shock wave formation difficult inside a collapsing bubble?

Answer 3.4

For the shock wave formation inside a collapsing bubble, the pressure wave radiated inwardly from the bubble wall into a collapsing bubble should overtake previously radiated pressure waves [22]. The speed of the propagation of the pressure wave is the sound speed plus the fluid velocity. Inside a collapsing bubble, the temperature increases as the distance from the bubble wall to the bubble center increases, due to thermal conduction between the colder bubble wall and the heated interior of the bubble. In general, the sound speed increases with temperature. This means that sound speed increases as the distance from the bubble wall to the bubble center increases (Figure 3.11). As a result, the pressure wave radiated inwardly from the bubble wall barely overtakes the previously radiated pressure waves. In other words, for many cases a shock wave is barely formed inside a collapsing bubble [23,24].

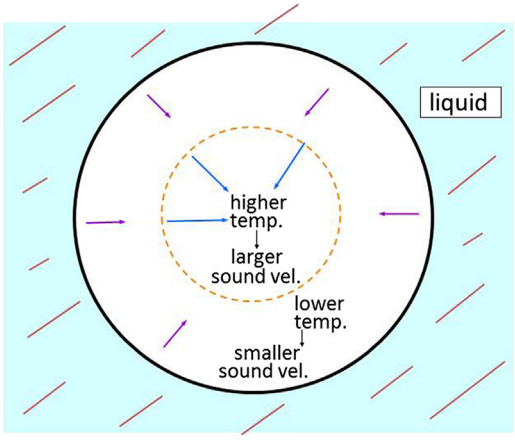

Figure 3.11
The difficulty in shock wave formation inside a collapsing bubble.

3.2.5 Transient and Stable Cavitation

There are two major categories of acoustic cavitation [4]; one is transient cavitation, and the other is stable cavitation. The definition of each category, however, is not absolute. One definition is based on the stability (lifetime) of cavitation bubbles. In transient cavitation, a bubble disintegrates into daughter bubbles in one or a few acoustic cycles. The daughter bubbles dissolve into the liquid due to the high (Laplace) pressure inside the bubbles, or coalesce with each other to form a larger active bubble. (When a daughter bubble is not too small, it may be an active bubble by itself without coalescence with other bubbles). In stable cavitation, bubbles stably pulsate. This is especially true for bubbles visible to the naked eye, which are usually larger than a few hundred micrometers and are very stable because they mildly pulsate [25].

The other definition is based on the activity of the bubbles. In transient cavitation, bubbles are active in sonoluminescence (light emission) or sonochemical reactions due to the Rayleigh collapse. In stable cavitation, bubbles are inactive.

A SBSL bubble is both active in sonoluminescence and stable with a very long lifetime. Thus, such a cavitation bubble is either transient or stable depending on the definition. Based on its stability, the acoustic bubble is called high-energy stable cavitation. Based on its activity, the acoustic bubble can be referred to as repetitive transient cavitation [2,4]. It is necessary to designate which definition is used in a discussion using the term transient or stable cavitation.

3.2.6 Size of an Active Bubble

First, the resonance frequency of a bubble is discussed (Minnaert Eqn (2.53)). In general, temporal variation of the bubble radius is described in the form of Eqn (3.42):

$$R(t) = R_0(1 + x(t)) \tag{3.42}$$

where R_0 is the equilibrium (ambient) bubble radius. In order to obtain the resonance radius of a bubble, $x(t)$ is regarded as less than 1 in magnitude, and the terms of higher order than 1 (x^2, x^3, …) are neglected. This is a linear approximation that implies that $R(t)$ temporally changes around R_0 in a smaller range than 0 to$2R_0$. Inserting Eqn (3.42) into the Rayleigh–Plesset Eqn (3.18), the linear approximation yields Eqn (3.43):

$$\ddot{x} + \alpha\dot{x} + \omega_0^2 x + \beta = A \sin \omega t \tag{3.43}$$

where α, ω_0, β, and A are constants, and ω is the angular frequency of the driving ultrasound. The resonance angular frequency of a bubble, ω_0, is approximately expressed by Eqn (3.44), which is equivalent to Eqn (2.53):

$$\omega_0 = \frac{1}{R_0}\sqrt{\frac{3\gamma p_0}{\rho}} \tag{3.44}$$

where the bubble pulsation is assumed to be adiabatic (Eqn (3.45)):

$$p_g = \left(p_0 + \frac{2\sigma}{R_0}\right)\left(\frac{R_0}{R}\right)^{3\gamma} \tag{3.45}$$

where γ is the specific-heat ratio and σ is the surface tension. As $\gamma = 1.4$, $p_0 = 10^5$ N/m^2, and $\rho = 10^3$ kg/m^3 for an air bubble in water at 1 atm, relationship Eqn (3.46) holds between the resonance frequency f_0 and radius R_0:

$$f_0 R_0 \approx 3 \tag{3.46}$$

For example, the resonance frequency of an air bubble of $R_0 = 3$ μm is about 1 MHz. For more accurate calculations, Eqn (3.47) is used [4]:

$$\omega_0 = \frac{1}{R_0}\sqrt{\frac{1}{\rho}\left(3\gamma p_0 + \frac{2\sigma}{R_0}(3\gamma - 1)\right)} \tag{3.47}$$

In summary, the resonance frequency or resonance radius is defined based on a linear approximation of the relevant equations. In other words, the Minnaert Eqn (3.44) (or Eqns. (3.46) and (3.47)) is useful only when the bubble pulsation is mild ($|x|<1$). In general, under the conditions for the Rayleigh collapse, a bubble dramatically expands before the collapse, and the condition ($|x|<1$) is not satisfied. Thus, a bubble at its resonance size is not necessarily an active bubble.

What is the upper limit of the acoustic pressure-amplitude for the condition ($|x|<1$) to hold? The relationship between the ambient bubble radius and the expansion ratio (maximum radius divided by ambient radius) is shown in Figure 3.12 for various acoustic pressure-amplitudes (A) [26]; these are the numerical simulation results of the Keller equation under 300 kHz ultrasound. According to the Minnaert equation, the resonance radius of a bubble at 300 kHz is about 10 μm. This means that the peak of the expansion ratio should be at around 10 μm in ambient radius if the bubble pulsation is sufficiently mild. According to Figure 3.12, however, even at an acoustic pressure-amplitude of 0.5 bar (about 0.5 atm), the peak appears at smaller ambient radius than 10 μm. Even at this relatively low acoustic pressure-amplitude, the linear resonance radius given by the Minnaert equation is overestimated. As the acoustic pressure-amplitude increases further, the ambient radius at the peak deviates further from the resonance radius. (At 3 bar, it is 0.4 μm, or about two orders of magnitude smaller than the resonance radius.) This is caused by the strong nonlinear pulsation of a bubble where higher order terms x^2, x^3, … become significant as a result of the large radial expansion of the bubble.

In general, the ambient radius for an active bubble that experiences Rayleigh collapse ranges from the Blake threshold radius (Figure 3.6 or Eqn (3.10)) to the linear resonance radius (Eqn (3.44) or (3.47)), based on numerical simulations of the Keller equation [26].

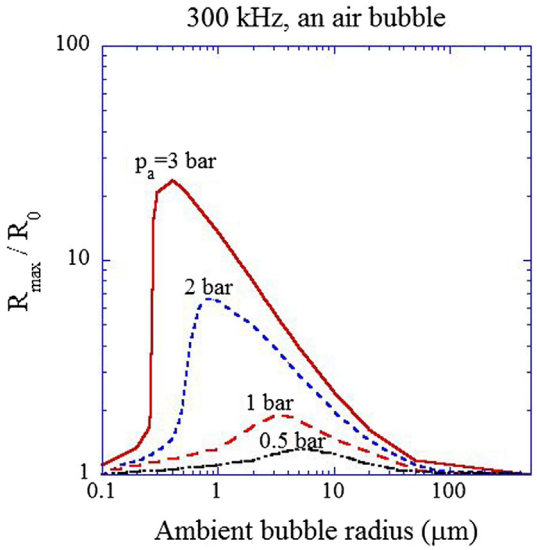

Figure 3.12

The expansion ratio as a function of ambient (equilibrium) bubble radius. (The results are from numerical simulations.) The ultrasonic frequency is 300 kHz. The acoustic pressure-amplitude is also shown in the figure. *Reprinted with permission from Ref. [26]. Copyright 2008, AIP Publishing LLC.*

3.2.7 Acoustic Cavitation Noise

During acoustic cavitation experiments undertaken in a laboratory, one can often recognize weak audible noise attributable to cavitation bubbles. A loudspeaker for music radiates sound by the vibration of its diaphragm. Similarly, a bubble radiates sound due to its vibration (pulsation). The sound radiated by pulsating bubbles in acoustic cavitation is known as acoustic cavitation noise.

The experimental data of the frequency spectra of acoustic cavitation noise are shown in Figure 3.13 for various intensities of ultrasound [27]. For the conditions shown in the figure as a and b, the signal is mostly ultrasound itself at 515 kHz, with almost negligible acoustic cavitation noise. At the threshold for sonoluminescence and sonochemical reactions (condition c), there are small peaks at harmonics (integer multiples of the fundamental frequency) of 515 kHz. For conditions d–f, subharmonic (fundamental frequency divided by an integer), ultraharmonic (integer multiples of subharmonics excepting harmonics), and broadband noise (the continuum part of noise) are observed in addition to strong harmonics.

Acoustic cavitation noise is strongly influenced by a small amount of surfactant. When the concentration of sodium dodecyl sulfate (SDS) is in the range 0.5–2 mM, subharmonic, ultraharmonic, and broadband noise are strongly weakened [27]. Above 3 mM, the acoustic cavitation noise from an aqueous SDS solution is almost the same as that from pure water.

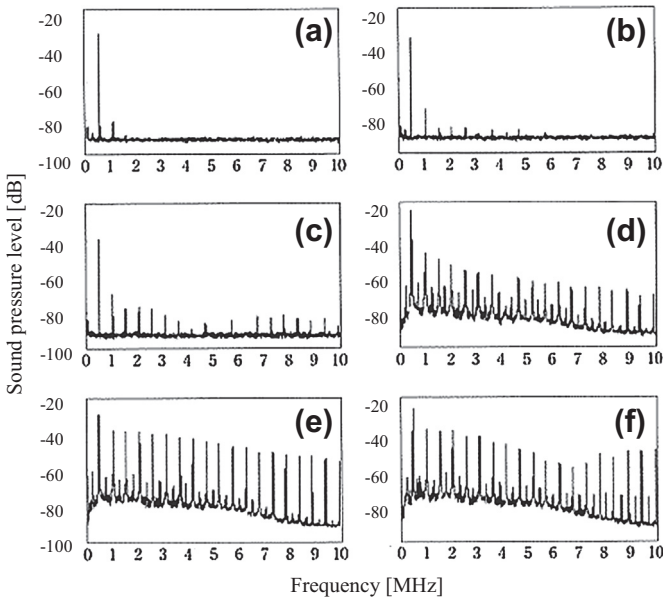

Figure 3.13

Acoustic emission spectra observed from water irradiated with ultrasound of 515 kHz from the bottom of a liquid container at different applied acoustic intensities as determined by calorimetry: (a) 0.05 W/cm^2, (b) 0.08 W/cm^2, (c) 0.54 W/cm^2 (above this level, significant sonochemistry and sonoluminescence emission occurred), (d) 0.7 W/cm^2, (e) 2.2 W/cm^2, and (f) 6.8 W/cm^2. *Reprinted with permission from Ref. [27]. Copyright (2007) American Chemical Society.*

In an aqueous SDS solution at low concentrations, bubble–bubble coalescence is strongly retarded, and consequently most of the bubbles are much smaller than those in pure water [28]. The retardation of bubble coalescence is a consequence of the electrostatic repulsion between bubbles that are covered with the ionic surfactant. The small bubbles in an SDS solution are mostly shape-stable, because nonspherical oscillations of a bubble are weaker for a smaller bubble. (Strong nonspherical oscillations lead to the fragmentation of a bubble.) In other words, in low-concentration SDS solutions, the high-energy stable cavitation discussed in Section 3.2.5 occurs. Consequently, the temporal periodicity of the acoustic emissions from bubbles is improved compared with that in pure water. This results in the emission of harmonics and the absence of subharmonic, ultraharmonic, and broadband noise [29]. Known in mathematics as a Fourier series, the spectrum of an arbitrary periodic function consists only of the fundamental frequency and its harmonics.

In an SDS solution with concentration above 3 mM, excess positive ions screen the negative charge on the bubble surface. This causes an increase in the extent of bubble coalescence and produces a larger number of bigger bubbles, compared with that in

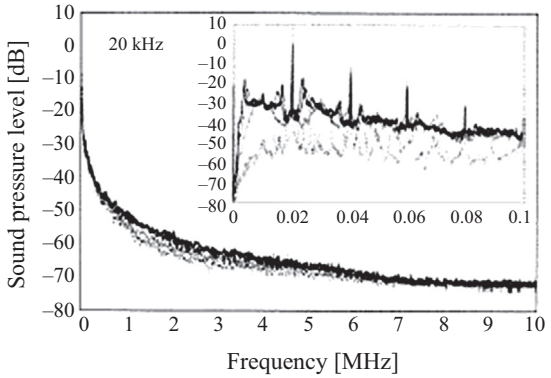

Figure 3.14

Acoustic emission spectra under an ultrasonic horn in water irradiated at 20 kHz at various acoustic intensities as determined by calorimetry: (dashed line) 10 W/cm^2, (gray line) 24 W/cm^2, (black line) 70 W/cm^2, and (heavy black line) 120 W/cm^2. Inset shows emission between 0 and 100 kHz. *Reprinted with permission from Ref. [30]. Copyright (2005) American Chemical Society.*

low-concentration SDS solutions. Then, more bubbles fragment into daughter bubbles, and the irregular temporal variation of the acoustic emission is intensified due to the temporal fluctuation in the number of bubbles. This results in a much stronger broadband acoustic noise [29]. Relatively large bubbles pulsate with a doubled period, resulting in subharmonic and ultraharmonic emissions.

However, there are other hypotheses to explain the observations. For example, it may be that nonperiodic (chaotic) pulsation of relatively large bubbles results in broadband noise. Nonlinear propagation of ultrasound in a bubbly liquid may also result in broadband noise. Subharmonic emission may be due to the nonspherical oscillation of a bubble. Further studies are required on the subject.

The acoustic cavitation noise under an ultrasonic horn is quite different from that in a bath-type reactor. The broadband noise is stronger under a horn, while harmonics are much weaker (Figure 3.14) [30].

3.3 Growth or Dissolution of a Bubble

3.3.1 Nucleation of a Bubble at a Solid Surface

The cavitation threshold depends not only on the gas concentration in the liquid (Figure 3.3), but also on the concentration of impurities. For example, the cavitation threshold of more than 22 bar at 750 kHz with pulsed ultrasound of 1% duty cycle (=1% on-time with 99% off-time) decreases to less than 10 bar with the addition of an appropriate amount of silica (SiO_2) microparticles [31].

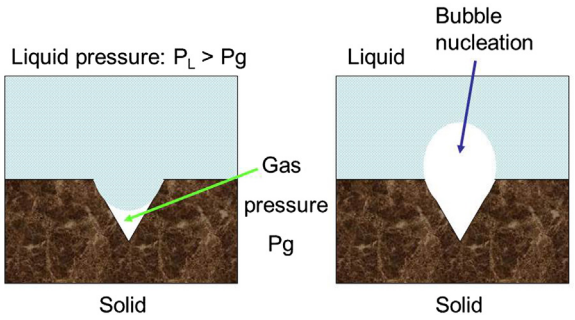

Figure 3.15
Mechanism for bubble nucleation at a solid (particle) surface.

One of the reasons for the decrease in the cavitation threshold by the addition of particles is the nucleation of bubbles at crevices on the surface of particles (Figure 3.15). In a crevice, the gas–liquid interface becomes concave, and the Laplace pressure makes the internal gas pressure lower than the liquid pressure. As a result, gas dissolution into the surrounding liquid is strongly retarded. On a hydrophobic surface of a solid, the radius of curvature of the gas–liquid interface is smaller than that on a hydrophilic surface. Thus, in a crevice on a hydrophobic surface, the Laplace pressure is stronger, and the gas dissolution is more strongly retarded. Indeed, there are several experimental reports indicating that more bubbles are created on hydrophobic surfaces than on hydrophilic ones [32].

Under ultrasound, gas in a crevice expands during the rarefaction phase, and the gas pressure further decreases, causing the diffusion of the gas in the surrounding liquid into the crevice. As a result, the volume of gas in the crevice gradually increases. Finally, a new bubble moves upward from the crevice, by buoyancy or radiation forces, when the volume of gas in the crevice becomes large enough. Bubbles pinch off, leaving behind bubble nuclei, and new bubbles are successively emitted from the crevice in this manner.

3.3.2 Dissolution of a Bubble

The internal gas pressure of a spherical bubble is higher than the pressure of the surrounding liquid by the Laplace pressure, due to surface tension in the absence of ultrasound. As a result, gas gradually dissolves into the surrounding liquid. An air bubble of 10 μm radius completely dissolves into air-saturated liquid in 6.6 s [2]. In degassed water, the time is only 1.2 s. In water in which the air is dissolved by 50% of the saturation value, the time is 2 s.

Question 3.5

What is the time for the complete dissolution of a bubble?

Answer 3.5

The dissolution of a gas bubble in the absence of ultrasound is described by the diffusion equation:

$$\frac{\partial C}{\partial t} = D\left(\frac{\partial^2 C}{\partial r^2} + \frac{2}{r}\frac{\partial C}{\partial r}\right) \tag{3.48}$$

where C is the gas concentration in the liquid, t is time, r is the distance from the bubble center, D is the diffusion coefficient of gas in the liquid, and the transport term, $V\partial C/\partial r$, where V is the velocity produced in the liquid by bubble growth or shrinkage, has been omitted from the left-hand side of Eqn (3.48). The solution of the diffusion equation is given as follows [33,34]:

$$\left(\frac{\partial C}{\partial r}\right)_R = (c_i - c_s)\left(\frac{1}{R} + \frac{1}{\sqrt{\pi D t}}\right) \tag{3.49}$$

where R is the bubble radius, c_i is the gas concentration in the liquid far from the bubble, and c_s is the saturated gas concentration at the bubble wall. Then, the gas flow into the bubble per unit time is given as follows (the gas flow out of a bubble is expressed by a negative value):

$$\frac{dm}{dt} = 4\pi R^2 D\left(\frac{\partial C}{\partial r}\right)_R = 4\pi R^2 D(c_i - c_s)\left(\frac{1}{R} + \frac{1}{\sqrt{\pi D t}}\right) \tag{3.50}$$

The equation of state for a gas bubble is expressed as follows, taking into account the Laplace pressure due to surface tension:

$$p_\infty + \frac{2\sigma}{R} = \frac{R_g}{M}\rho(R)T \tag{3.51}$$

where p_∞ is the pressure of the liquid, σ is the surface tension, R_g is the universal gas constant, M is the molar weight of the gas, $\rho(R)$ is the gas density inside the bubble, and T is the temperature inside the bubble. Then, the following relationship holds:

$$\rho(R) = \frac{M}{R_g T}p_\infty + \frac{2M\sigma}{R_g T}\frac{1}{R} = \rho(\infty) + \frac{\tau}{R} \tag{3.52}$$

where $\rho(\infty)$ is the density of gas under the same conditions of pressure and temperature with a gas–liquid interface of zero curvature, and

$$\tau = \frac{2M\sigma}{R_g T} \tag{3.53}$$

Then, the mass of gas in the bubble is expressed as follows:

$$\mathrm{m} = \frac{4\pi}{3}R^3\rho(R) = \frac{4\pi}{3}R^3\rho(\infty) + \frac{4\pi}{3}R^2\tau \tag{3.54}$$

Its time derivative is expressed as follows:

$$\frac{dm}{dt} = 4\pi R^2 \frac{dR}{dt}\left(\rho(\infty) + \frac{2\tau}{3R}\right) \tag{3.55}$$

The equality of Eqns (3.50) and (3.55) yields the following differential equation for the bubble radius (R):

$$\frac{dR}{dt} = \frac{D(c_i - c_s)}{\rho(\infty) + 2\tau/3R}\left(\frac{1}{R} + \frac{1}{\sqrt{\pi Dt}}\right) \tag{3.56}$$

Here, the quantities d and f are introduced by the following definitions [33]:

$$d = \frac{c_s}{\rho(R)} = \frac{c_s}{\rho(\infty) + \tau/R} \tag{3.57}$$

$$f = \frac{c_i}{d\rho(\infty)} = \frac{c_i\rho(R)}{c_s\rho(\infty)} \tag{3.58}$$

When the liquid is saturated with gas, $f = 1$ holds because $c_s\rho(\infty)/\rho(R)$ is equivalent to the saturated gas concentration far from the bubble. Using the quantities d and f, Eqn (3.56) is expressed as follows:

$$\frac{dR}{dt} = -Dd\frac{1 - f + \tau/(R\rho(\infty))}{1 + 2\tau/(3R\rho(\infty))}\left(\frac{1}{R} + \frac{1}{\sqrt{\pi Dt}}\right) \tag{3.59}$$

Now, the following dimensionless variables ε and x are introduced [33]:

$$\varepsilon = \frac{R}{R_0} \tag{3.60}$$

$$x^2 = \left(\frac{2Dd}{R_0^2}\right)t \tag{3.61}$$

Neglecting the second term in the bracket of Eqn (3.59) for nearly steady state ($t \to \infty$), Eqn (3.59) is expressed as follows:

$$\frac{d\varepsilon}{dx} = -\frac{1 - f + \frac{\delta}{\varepsilon}}{1 + \frac{2\delta}{3\varepsilon}}\left(\frac{x}{\varepsilon}\right) \tag{3.62}$$

where

$$\delta = \frac{\tau}{R_0\rho(\infty)} \tag{3.63}$$

The solution of Eqn (3.62) for $f = 1$ is given as follows:

$$\int \varepsilon^2\left(1 + \frac{2\delta}{3\varepsilon}\right)d\varepsilon = -\delta\int x dx \tag{3.64}$$

$$1 - \varepsilon^3 + \delta\left(1 - \varepsilon^2\right) = \frac{3\delta}{2}x^2 \tag{3.65}$$

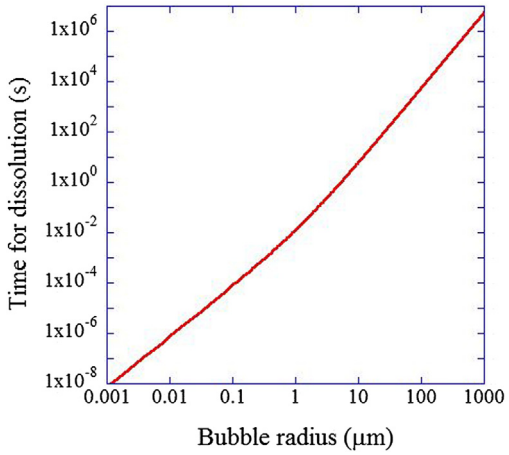

Figure 3.16
The time for complete dissolution of an air bubble in water saturated with air as a function of the bubble radius (R_0) calculated by Eqn (3.67).

where the initial condition ($\varepsilon = 1$ at $x = 0$) has been used. The time for the complete dissolution of a bubble ($\varepsilon = 0$) is derived from Eqn (3.65) as follows:

$$x^2 = \frac{2}{3\delta}(1+\delta) \tag{3.66}$$

It is rewritten as follows:

$$\mathrm{t} = \frac{1}{3}\left(1 + \frac{R_0 p_\infty}{2\sigma}\right)\left(\frac{R_0^2 M p_\infty}{D c_{s0} R_g T}\right) \tag{3.67}$$

where c_{s0} ($=c_s\rho(\infty)/\rho(R)$) is the saturated gas concentration in the liquid far from a bubble. The numerical result of Eqn (3.67) is shown in Figure 3.16 for an air bubble in air-saturated water at 20 °C ($p_\infty = 1$ atm $= 1.01325 \times 10^5$ Pa, $\sigma = 7.275 \times 10^{-2}$ N/m, $M = 28.96 \times 10^{-3}$ kg/mol, $D = 2.4 \times 10^{-9}$ m^2/s, $c_{s0} = 2.3 \times 10^{-2}$ kg/m^3, $R_g = 8.3145$ J/mol K, and $T = 293$ K). While a bubble with a 1 nm radius ($R_0 = 1 \times 10^{-9}$ m) completely dissolves into the liquid in 7 ns ($=7 \times 10^{-9}$ s), a bubble with a radius of 100 μm needs about 85 mins ($=5100$ s).

Equation (3.67) has been used in the experimental determination of the bubble size distribution under the sonoluminescence condition using pulsed ultrasound [28,35]. Larger bubbles need longer pulse-off time for complete dissolution and diminishing of the sonoluminescence intensity.

When a bubble's surface is covered by organic material or surfactant, gas diffusion is strongly retarded. Consequently, the lifetime of a bubble becomes much longer.
A nanobubble, defined as a bubble of less than 1 μm in radius, may have a relatively long lifetime when the bubble surface is covered by solid particles, organic materials, surfactants, etc. [36]. When the acoustic pressure-amplitude is relatively high, there are some nanobubbles larger than 100 nm in radius, in acoustic cavitation (Figures 3.6 and 3.12).

3.3.3 Bubble Nuclei

How are bubbles created when there are no solid particles in a liquid? First, even without adding solid particles, there are plenty of motes (dust particles) in a liquid. At crevices of motes, new bubbles are created under ultrasound (Figure 3.15). In addition, there are many crevices or scratches on the surface of a liquid container as well as on the tip of an ultrasonic horn. At such crevices (or scratches), new bubbles are created by the same mechanism as described in the previous section.

Secondly, there are many bubble nuclei (tiny bubbles or possibly nanobubbles) in a liquid. They have relatively long lifetimes because the surface is likely to be covered by dust particles, organic or inorganic impurities including surfactants, etc. These nuclei may coalesce with each other under ultrasound and become larger active bubbles.

The number concentration of bubble nuclei in liquid has been measured both optically and acoustically as 10^{-3} to 10^{2} cm^{-3}, depending on the amount and kind of impurities, as well as the condition of the water used, such as tap water, distilled water, static water, etc. [37]. The number concentration of bubbles in acoustic cavitation under ultrasound has been estimated to be greater than 10^{6} cm^{-3} [38].

3.3.4 Growth of a Bubble (Rectified Diffusion)

A bubble grows not only by coalescence of bubbles but also by gas diffusion into a bubble by a process called rectified diffusion. Rectified diffusion is based on an area effect and a shell effect, as discussed below [2]. During bubble expansion (when the instantaneous bubble radius is much larger than the ambient radius), the internal pressure of a bubble is lower than the partial pressure of gas dissolved in the surrounding liquid phase. As a result, gas diffuses into a bubble from the surrounding liquid. On the other hand, during bubble collapse (when the instantaneous bubble radius is comparable to or smaller than the ambient radius), the internal pressure of a bubble is higher than the partial pressure of gas dissolved in the liquid. As a result, gas diffuses out of the bubble into the surrounding liquid. When the amount of gas diffusing into a bubble is larger than that diffusing out of a bubble, the bubble will gradually grow.

The area effect is based on the fact that the amount of gas diffusing into or out of a bubble is proportional to the instantaneous surface area of a bubble. During bubble expansion, the surface area of a bubble is larger than that during bubble collapse. Thus the amount of gas diffusing into a bubble becomes larger than that diffusing out of a bubble due to this area effect. The shell effect is based on the fact that the amount of gas diffusing into or out of a bubble is proportional to the gradient of gas concentration in the liquid near the bubble surface. A spherical shell of constant volume surrounding a bubble becomes thinner during

the bubble expansion phase compared with that during bubble collapse. This implies that the gradient of gas concentration is larger during bubble expansion. Thus, the amount of gas diffusing into a bubble becomes larger than that diffusing out of a bubble by the shell effect, as well.

The growth rate of a bubble by rectified diffusion strongly depends on operating conditions, such as acoustic pressure-amplitude and acoustic frequency. At 20 kHz with an acoustic pressure-amplitude of 0.2 bar, the growth rate of a bubble of 35 μm in initial radius is a few μm per 100 s [39]. As the acoustic pressure-amplitude increases, the growth rate of the bubble dramatically increases. At an acoustic pressure-amplitude of 2 bar at 30 kHz, the growth rate ranges from 10 μm/s to several 100 μm/s depending on the initial bubble radius [40].

3.3.5 Growth of a Bubble (Coalescence)

Bubbles frequently coalesce with each other under ultrasound if the number concentration of bubbles is large enough. This is caused by an attractive force between bubbles called the secondary Bjerknes force given by Eqn (3.68) [41,42]. (The primary Bjerknes force is the ultrasonic radiation force on a bubble in a standing wave field as discussed in Section 3.4.1.)

$$\vec{F}_{1\to 2} = -\langle V_2 \nabla p_1 \rangle \tag{3.68}$$

where $\vec{F}_{1\to 2}$ is the force acting on bubble 2 from bubble 1, V_2 is the volume of bubble 2, p_1 is the acoustic pressure radiated from bubble 1, $\nabla = \left(\frac{\partial}{\partial x}, \frac{\partial}{\partial y}, \frac{\partial}{\partial z}\right)$, and $\langle\ \rangle$ means the time-averaged value.

Next, the acoustic pressure radiated by a pulsating bubble is discussed. Consider Euler's equation of motion for fluid dynamics (Eqn (3.69)):

$$\frac{\partial \vec{v}}{\partial t} + (\vec{v}\cdot\nabla)\vec{v} = -\frac{1}{\rho}\nabla p \tag{3.69}$$

where $\vec{v} = (v_x, v_y, v_z)$ is the fluid (liquid) velocity, $\vec{v}\cdot\nabla = v_x\frac{\partial}{\partial x} + v_y\frac{\partial}{\partial y} + v_z\frac{\partial}{\partial z}$, ρ is the liquid density, and p is the instantaneous local pressure of the liquid. The fluid (liquid) velocity $(\vec{v})$ around a pulsating bubble is given by Eqn (3.70) according to the condition for incompressibility of a liquid [the equation in brackets written below Eqn (3.11)]:

$$\vec{v} = \frac{R^2\dot{R}}{r^2}\vec{e}_r \tag{3.70}$$

where R is the instantaneous bubble radius, r is the distance from the bubble center, $\vec{e}_r$ is a unit vector in the direction from the bubble center to the observation point. Then, the

second term of the left side of Eqn (3.69) is proportional to r^{-5} and negligible compared with the first term. Thus, Eqn (3.71) is derived by inserting Eqn (3.70) into Eqn (3.69):

$$\frac{\partial p}{\partial r} = -\frac{\rho}{r^2}\frac{d}{dt}\left(R^2\dot{R}\right) \tag{3.71}$$

where p is the acoustic pressure radiated from a bubble; p is given by Eqn (3.72) by integrating Eqn (3.71) with r:

$$p = \frac{\rho}{r}\frac{d}{dt}\left(R^2\dot{R}\right) = \frac{\rho}{4\pi r}\frac{d^2V}{dt^2} \tag{3.72}$$

where $V = \frac{4\pi R^3}{3}$ is the volume of a bubble.

Finally, the secondary Bjerknes force is given by Eqn (3.73) by inserting Eqn (3.72) into Eqn (3.68):

$$\vec{F}_{1\to 2} = \frac{\rho}{4\pi d^2}\left\langle \ddot{V}_1 V_2 \right\rangle \vec{e}_{1\to 2} \tag{3.73}$$

where ρ is the liquid density, d is the distance between the bubble centers, $V_1(V_2)$ is the volume of bubble 1 (bubble 2), $\ddot{V}_1 = d^2V_1/dt^2$, and $\vec{e}_{1\to 2}$ is a unit vector in the direction from bubble 1 to bubble 2. When the coefficient of $\vec{e}_{1\to 2}$ is negative (positive), the secondary Bjerknes force is attractive (repulsive).

In Figure 3.17, numerical results of Eqn (3.73) are shown when the bubble pulsation is calculated by the Keller equation [42]. The horizontal (vertical) axis is the ambient radius

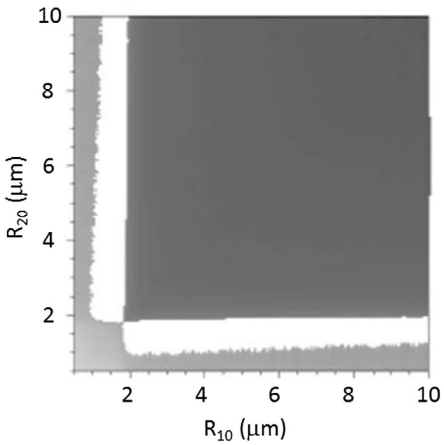

Figure 3.17

The relationship between the secondary Bjerknes force and the ambient (equilibrium) radius of two interacting bubbles (R_{10} and R_{20}). The white (black) color means that the force is repulsive (attractive). The darker the color, the stronger the attractive force. The frequency and pressure-amplitude of ultrasound in the numerical simulations are 20 kHz and 1.32 bar, respectively. The distance between the two bubbles is 1 mm. *Reprinted figure with permission from Ref. [42]. Copyright (1997) by the American Physical Society.*

of bubble 1 (bubble 2). When the secondary Bjerknes force is attractive (repulsive), the region is in black (white). In most cases, two pulsating bubbles will be attracted to each other through the secondary Bjerknes force. When one bubble is around 1 μm in ambient radius and much smaller than the other, two bubbles will repel each other due to the secondary Bjerknes force.

3.4 Interaction with the Surroundings

3.4.1 The Primary Bjerknes Force

The primary Bjerknes force is the ultrasonic radiation force on a pulsating bubble in a standing wave field of ultrasound given by Eqn (3.74) [41]:

$$\vec{F}_B = -\langle \vec{F}_p \rangle = -\langle V \nabla p \rangle \tag{3.74}$$

where $\vec{F}_p$ is the instantaneous radiation force on a bubble, $\langle\ \rangle$ means the time-averaged value, and V is the bubble volume. In a standing wave field, the acoustic pressure p is given by Eqn (3.75):

$$p(z,t) = -A\cos(kz)\sin(\omega t) \tag{3.75}$$

where A is the pressure-amplitude of ultrasound, $k = 2\pi/\lambda$ is the wave number, $\omega = 2\pi f$ is the angular frequency, and f is the ultrasonic frequency. When a liquid is irradiated with ultrasound by a transducer attached at the bottom ($z = 0$) of the liquid container, a standing wave field given by Eqn (3.75) is formed if the liquid height is at $z = (2n + 1)\pi/2k$, where the z-axis is in the vertical direction and n is a natural number. Then, the primary Bjerknes force is given by Eqn (3.76):

$$\vec{F}_p = \left(-4\pi/3\right)R^3 kA\,\sin(kz)\sin\left(\omega t\right)\vec{e}_z \tag{3.76}$$

where R is the instantaneous bubble radius and $\vec{e}_z$ is a unit vector in z direction.

In Figure 3.18(a), the bubble radius as well as the instantaneous radiation pressure is shown as a function of time at 20 kHz [43]. A bubble is slightly off the pressure antinode ($cos(kz) = \pm 1$) in the calculation. During the rarefaction phase of an ultrasound wave, over the initial half-wave period (0−25 μs), a bubble expands. At this stage, the instantaneous acoustic pressure is lowest at the pressure antinode, and the instantaneous radiation force is directed toward the pressure antinode. (The instantaneous radiation force is always directed toward the lower pressure region as Eqn (3.74).) In the compression phase of ultrasound during the latter half wave period (25−50 μs), a bubble collapses and undergoes repeating small pulsations. At this stage, the instantaneous acoustic pressure is highest at the pressure antinode, and the instantaneous radiation force is directed away from the pressure antinode.

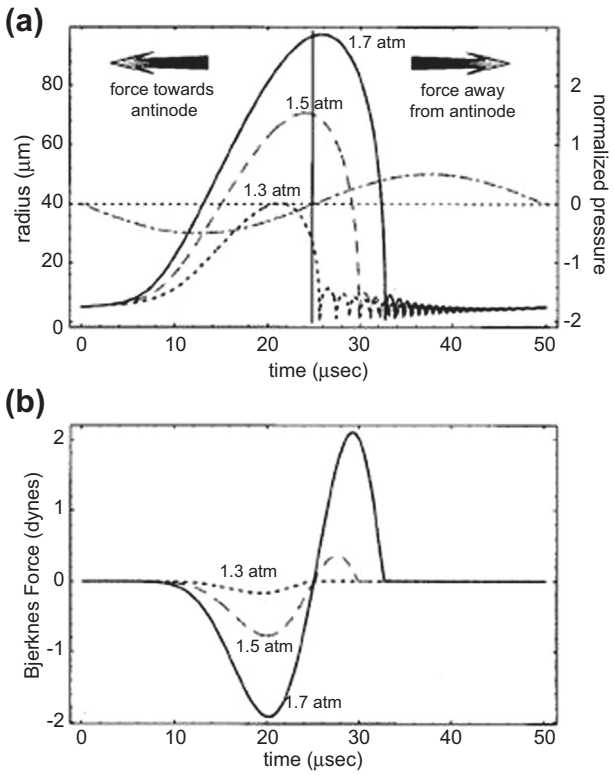

Figure 3.18

The primary Bjerknes force. (a) Calculated radius–time curve for one acoustic cycle. The ultrasonic frequency is 20 kHz. The acoustic pressure-amplitude is 1.3, 1.5, and 1.7 atm going from bottom to top. The ambient (equilibrium) bubble radius is 5 μm. (b) Calculated instantaneous primary Bjerknes force as a function of time. A negative value means that the force is directed toward the pressure antinode. *Reprinted with permission from Ref. [43]. Copyright (1997), Acoustical Society of America.*

As the instantaneous radiation force is proportional to the volume of a bubble (Eqn (3.74)), the force is stronger during bubble expansion compared with that during bubble collapse. As a result, the time-averaged value in Eqn (3.74) is directed toward the pressure antinode. However, above about 1.8 bar in acoustic pressure-amplitude at 20 kHz, bubble expansion still takes place at the beginning of the compression phase of the ultrasound wave. This gives rise to a repulsive force from the pressure antinode in the compression phase that is stronger than the attractive one generated during the rarefaction phase. Consequently, above about 1.8 bar at 20 kHz, a bubble is repelled from the pressure antinode.

This means that a bubble does not enter the noted region above about 1.8 bar for an acoustic pressure-amplitude at 20 kHz. In fact, bubbles gather around the plane between

the pressure node and antinode in the fluid, when the acoustic pressure-amplitude at an antinode is higher than the critical one (1.8 bar at 20 kHz) (Figure 3.19) [41]. Such a spatial structure of bubbles is known as the jellyfish structure (or the double-layer structure).

When the ambient bubble radius is larger than the resonance radius, bubble pulsation is in an antiphase mode relative to the ultrasound wave. In this case, a bubble expands during the compression phase of the ultrasound, and the time-averaged radiation force is directed away from the pressure antinode. Thus, such large bubbles are trapped at pressure nodes in the fluid.

3.4.2 Bubble Collapse Near a Solid Surface

When a bubble expands and subsequently collapses near a solid surface, the liquid pressure at the bubble surface away from the solid wall becomes higher than that near the wall. As a result, a liquid jet penetrates into the bubble and is directed toward the solid wall (Figures 3.20 and 3.21) [44,45]. The rapidly moving liquid jet (>200 m/s) hits the

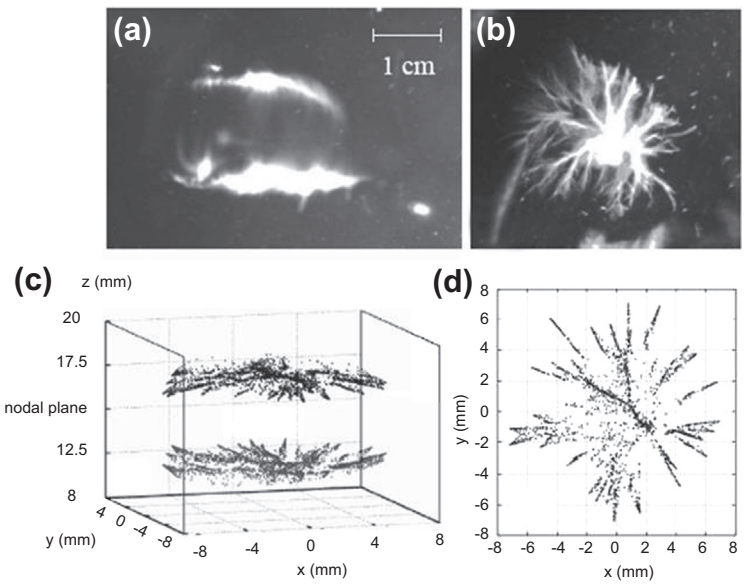

Figure 3.19

A jellyfish (double-layer) structure of acoustic cavitation bubbles in a standing wave field of ultrasound at 25 kHz. The acoustic pressure-amplitude at the antinode is about 2 atm. The photographs are from the side (a) and the top (b). Results of particle model simulations for the side view (c) and the top view (d). *Reprinted with permission from Ref. [41]. Copyright (2005), Research Signpost.*

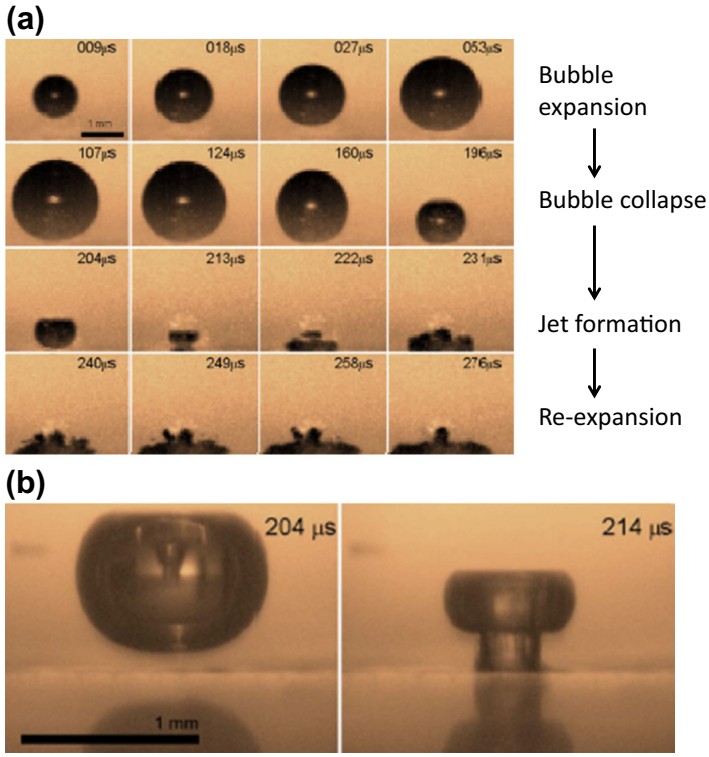

Figure 3.20
Bubble collapse near a solid surface. A bubble was formed in water near a solid surface by high intensity laser light irradiation at time 0. (a) The images were taken with a high-speed camera. The bar in the top-left image corresponds to 1 mm. (b) Stroboscopic pictures visualize the liquid jet within the bubble (left) and its impact on the substrate (right). The bar in the left picture corresponds to 1 mm. *Reprinted with permission from Ref. [44]. Copyright (2006), AIP Publishing LLC.*

solid surface, and this may result in ultrasonic cleaning of the surface and/or cavitation damage to the solid substrate. In Figure 3.22, jet impacts were recorded on a solid surface fouled with microparticles appearing as circular spots [46].

3.4.3 Emission of a Shock Wave into a Liquid

When a bubble violently collapses, a spherical shock wave is emitted from the bubble. In Figure 3.23, a spherical shock wave is seen as a ring [47]. At the center of the ring, there is actually a bubble from which the shock wave was emitted, although it is invisible in the photograph.

The cause of shock wave formation is as follows. A shock wave is formed when a pressure wave progressively overtakes previously radiated pressure waves. At the

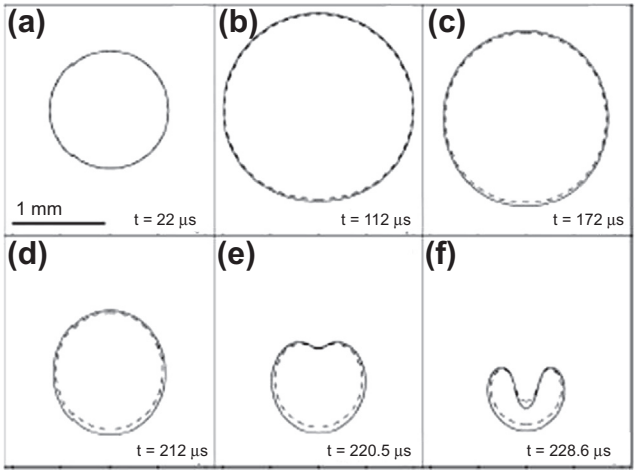

Figure 3.21

The results of numerical simulations on bubble pulsations near a solid surface in water (solid line) or oil (dashed line). The solid surface is at the bottom of each figure. The bar in the top-left figure corresponds to 1 mm. *Reprinted figure with permission from Ref. [45]. Copyright (2009), AIP Publishing LLC.*

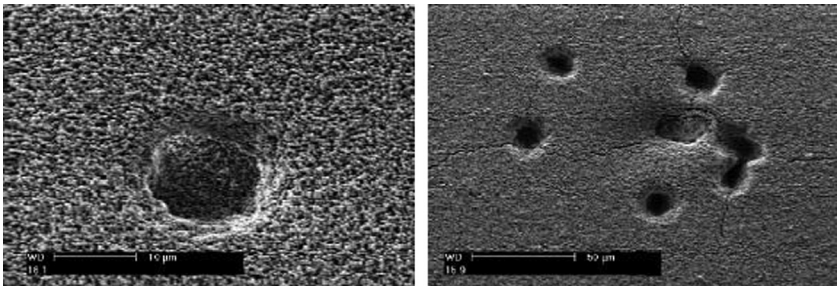

Figure 3.22

Scanning Electron Microscope (SEM) images showing evidence of microjet impacts on the surface of a fouling-cake layer (fouled with 0.5 μm sulfate—polystyrene particles). Left: ultrasound of 1062 kHz and 0.21 W/cm^2 for 5 s. The scale bar corresponds to 10 μm. Right: ultrasound of 620 kHz and 0.12 W/cm^2 for 5 s. The scale bar corresponds to 50 μm. *Reprinted from Ref. [46]. Copyright (2004), with permission from Elsevier.*

beginning of a bubble expansion, just after a strong collapse of a bubble, the liquid velocity near the bubble wall is directed outward, and decreases in amplitude with increasing distance from the bubble [48]. Far from the bubble, the liquid velocity is still directed toward the bubble at this moment. The speed of the bubble expansion gradually increases with time. As the propagation speed of a pressure wave is the sum of the local

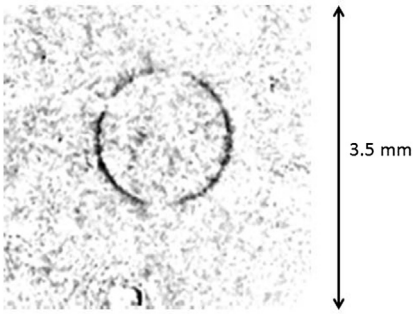

Figure 3.23
Image of a spherical shock wave emitted from a sonoluminescing bubble with a video camera at 480 ns after bubble collapse. The bubble is at the center of the circle, although it is invisible in the image. *Reprinted figure with permission from Ref. [47]. Copyright (1998) by the American Physical Society.*

instantaneous liquid velocity and the sound speed, a pressure wave radiating outward from a bubble progressively overtakes the previously radiated pressure wave. Finally, a spherical shock wave is formed.

3.4.4 Acoustic Streaming and Microstreaming

An acoustic wave (ultrasonic wave) often causes fluid (liquid or gas) streaming. There are basically two mechanisms. One is the case of a traveling acoustic wave. In this case, attenuation of a traveling wave (mostly due to the viscosity of the liquid) causes the streaming. Without attenuation, the time-averaged force on a liquid particle moving forward and backward periodically with respect to time is zero. This is because the force pushing and pulling a liquid particle is the same in its amplitude and symmetric around zero with respect to time, as the amplitude of the force is independent of the spatial position. On the other hand, with some attenuation of an acoustic wave, the pushing force is stronger than the pulling one because of the decrease in the acoustic pressure-amplitude in the direction of acoustic-wave propagation. As a result, the liquid is accelerated in the direction of the wave propagation. Thus, the speed of the streaming flow increases with distance in the direction of the wave propagation.

The other mechanism is associated with the effect of boundaries, such as a container's wall or bubbles. In this case, the frictional force at the boundaries causes streaming irrespective of the situation of a traveling or standing wave. An example of this category is microstreaming around a bubble (or a solid particle).

The fluid flow in the former category, as well as that in the latter one, such as large vortexes in a standing wave field, is called acoustic streaming [49]. The length scale for

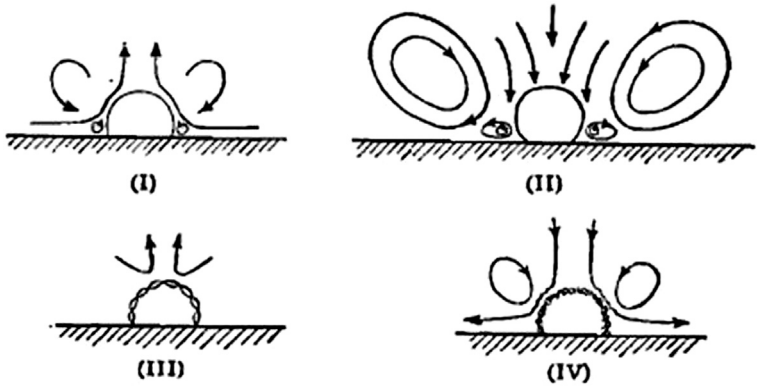

Figure 3.24
Four types of microstreaming around a bubble. *Reprinted with permission from Ref. [51]. Copyright (1959), Acoustical Society of America.*

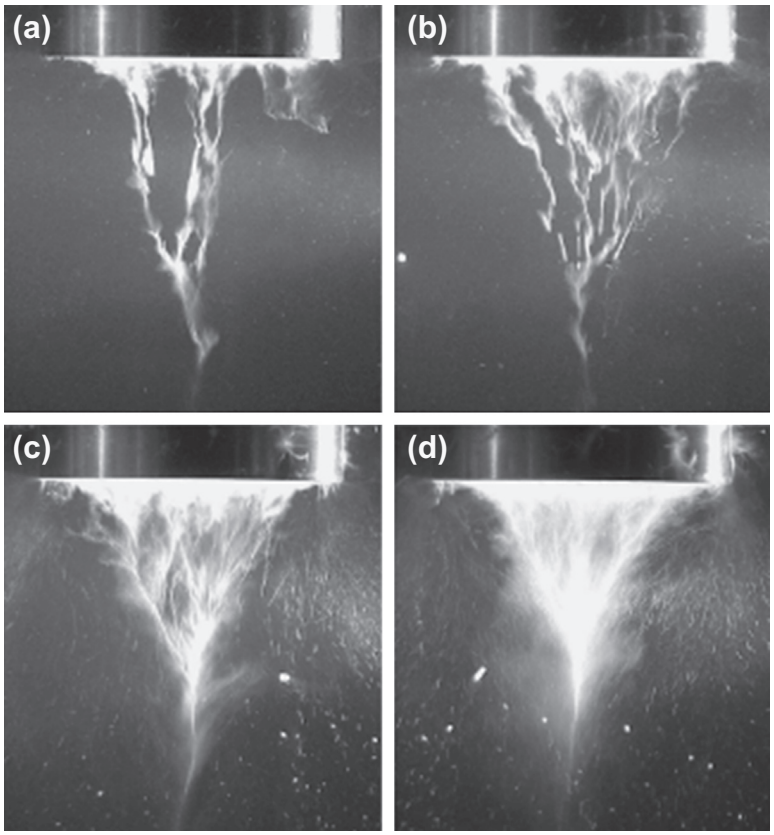

Figure 3.25
Images of cavitation bubbles under an ultrasonic horn at 20.7 kHz, obtained using a digital photo camera. The acoustic intensity was (a) 1.8, (b) 3.5, (c) 5.3, and (d) 8.2 W/cm^2. The diameter of the horn is 120 mm. *Reprinted from Ref. [52]. Copyright (2003), with permission from Elsevier.*

acoustic streaming is greater than the order of the acoustic wavelength, whereas that for microstreaming is usually less than 1 mm and only near a bubble (or solid particle).

While microstreaming occurs not only around a bubble but also around a solid particle, it is especially significant around a pulsating bubble because the speed of microstreaming is proportional to the square of the vibration speed of the object. The speed of microstreaming is on the order of $U^2/\omega a$, where U is the vibration speed of the object (vibration speed of a pulsating bubble, or that of a solid particle due to an acoustic wave), ω is the angular frequency of the acoustic wave, and a is the radius of the object [50]. The speed of microstreaming around a pulsating bubble is 10^2–10^6 times larger than that around a solid particle. Thus, the term "microstreaming" is usually used for the liquid streaming around a pulsating bubble. In Figure 3.24, some examples of the pattern of microstreaming around a pulsating bubble on a solid surface are shown [51].

The actual liquid flow from acoustic cavitation is highly complex. Firstly, ultrasound is strongly attenuated by cavitation bubbles, and acoustic streaming is intensified. In addition, bubbles move due to primary and secondary Bjerknes forces. The drag forces associated with the movement of bubbles cause further liquid flow. The liquid flow and the movement of bubbles influence each other in complex ways. In Figure 3.25, bubbles under an ultrasonic horn are shown [52]. While many bubbles move away from the horn tip, some others move toward it [38]. The liquid (water) flows downward at about 2 m/s near the horn tip, and the liquid speed decreases with the distance from the horn tip [53]. Details of the bubble motion as well as the liquid flow under an ultrasonic horn are unknown at present due to this complexity.

3.4.5 Interaction with Neighboring Bubbles

Neighboring bubbles influence the pulsation of a bubble primarily in three ways. One is the scattering and reflection of ultrasound by neighboring bubbles. This results in a decrease in the acoustic pressure-amplitude. This effect is called the screening of ultrasound. Another is nonspherical bubble collapse due to the presence of neighboring bubbles. For example, a liquid jet projects toward another bubble in a system of two bubbles (Figure 3.26) [54]. This is observed when the acoustic pressure-amplitude is relatively high. The other is the influence of acoustic waves radiated by neighboring bubbles on the pulsation of a bubble. As discussed in Section 3.2.7, pulsating bubbles radiate acoustic waves into the surrounding liquid. The radiated acoustic waves strongly suppress nearby bubble expansion, which is called the bubble–bubble interaction (Figure 3.27) [38]. There is also the case that shock waves emitted from neighboring bubbles accelerate neighboring bubble collapse [55].

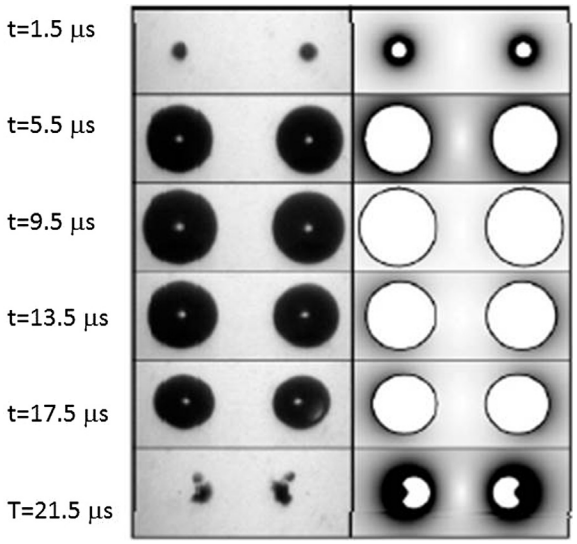

Figure 3.26

The pulsation of two bubbles initially set apart at a distance of 400 μm subjected to a minimum pressure of −1.4 MPa (the pulse width is about 4 μs). Left: experiment, right: numerical simulation. *Reprinted with permission from Ref. [54]. Copyright (2006), AIP Publishing LLC.*

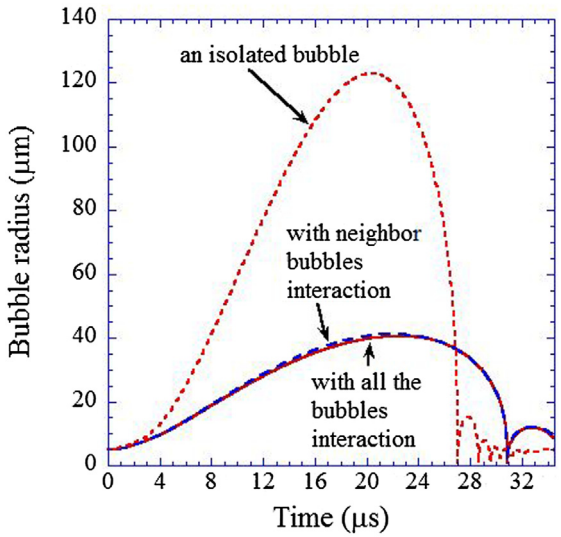

Figure 3.27

The results of numerical simulations of bubble pulsation in water under ultrasound of 29 kHz and 2.36 bar for frequency and pressure-amplitude, respectively. *Reprinted figure with permission from Ref. [38]. Copyright (2008) by the American Physical Society.*

References

[1] F.R. Young, Cavitation, Imperial College Press, London, 1999.
[2] T.G. Leighton, The Acoustic Bubble, Academic Press, London, 1994.
[3] E.A. Neppiras, Acoustic cavitation, Phys. Rep. 61 (1980) 159–251.
[4] K. Yasui, Fundamentals of acoustic cavitation and sonochemistry, in: Pnkaj, M. Ashokkumar (Eds.), Theoretical and Experimnetal Sonochemistry Involving Inorganic Systems, Springer, Dordrecht, 2011, pp. 1–29 (Chapter 1).
[5] Y. Lecoffre, in: V.H. Arakeri (Ed.), Cavitation, Bubble Trackers, A.A.Balkema Pub., Rotterdam, 1999 translated by M.M.Oberai, transl.
[6] W.J. Galloway, An experimental study of acoustically induced cavitation in liquids, J. Acoust. Soc. Am. 26 (1954) 849–857.
[7] P. Atkins, J.d. Paula, Atkins' Physical Chemistry, ninth ed., Oxford Univ. Press, Oxford, 2010 (Chapter 17), pp. 622–658.
[8] A. Prosperetti, A. Lezzi, Bubble dynamics in a compressible liquid. Part I. First-order theory, J. Fluid Mech. 168 (1986) 457–478.
[9] I. Akhatov, O. Lindau, A. Topolnikov, R. Mettin, N. Vakhitova, W. Lauterborn, Collapse and rebound of a laser-induced cavitation bubble, Phys. Fluids 13 (2001) 2805–2819.
[10] S. Müller, M. Bachmann, D. Kroninger, T. Kurz, P. Helluy, Comparison and validation of compressible flow simulations of laser-induced cavitation bubbles, Comput. Fluids 38 (2009) 1850–1862.
[11] L. Rayleigh, On the pressure developed in a liquid during the collapse of a spherical cavity, Phil. Mag 34 (1917) 94–98.
[12] P.M. Morse, H. Feshbach, Methods of Theoretical Physics, Part I, McGraw-Hill, New York, 1953.
[13] H. Gould, J. Tobochnik, W. Christian, An Introduction to Computer Simulation Methods, Applications to Physical Systems, third ed., Pearson, Addison Wesley, San Francisco, 2007.
[14] W.H. Press, S.A. Teukolsky, W.T. Vetterling, B.P. Flannert, Numerical Recipes, The Art of Scientific Computing, third ed., Cambridge Univ. Press, New York, 2007 (Chapter 17), pp. 899–954.
[15] D.F. Griffiths, D.J. Higham, Numerical Methods for Ordinary Differential Equations, Initial Value Problems, Springer, London, 2010.
[16] K. Yasui, T. Tuziuti, T. Kozuka, A. Towata, Y. Iida, Relationship between the bubble temperature and main oxidants created inside an air bubble under ultrasound, J. Chem. Phys. 127 (2007) 154502.
[17] M.P. Brenner, S. Hilgenfeldt, D. Lohse, Single-bubble sonoluminescence, Rev. Mod. Phys. 74 (2002) 425–484.
[18] K. Yasui, Alternative model of single-bubble sonoluminescence, Phys. Rev. E 56 (1997) 6750–6760.
[19] K. Yasui, Effect of liquid temperature on sonoluminescence, Phys. Rev. E 64 (2001) 016310.
[20] K. Yasui, K. Kato, Bubble dynamics and sonoluminescence from helium or xenon in mercury and water, Phys. Rev. E 86 (2012) 036320, 069901(E).
[21] Y. An, Mechanism of single-bubble sonoluminescence, Phys. Rev. E 74 (2006) 026304.
[22] V.Q. Vuong, A.J. Szeri, D.A. Young, Shock formation within sonoluminescence bubbles, Phys. Fluids 11 (1999) 10–17.
[23] H.Y. Chen, M.-C. Chu, P.T. Leung, L. Yuan, How important are shock waves to single-bubble sonoluminescence? Phys. Rev. E 58 (1998) R2705–R2708.
[24] L. Yuan, H.Y. Cheng, M.-C. Chu, P.T. Leung, Physical parameters affecting sonoluminescence: a self-consistent hydrodynamic study, Phys. Rev. E 57 (1998) 4265–4280.
[25] K. Yasui, Influence of ultrasonic frequency on multibubble sonoluminescence, J. Acoust. Soc. Am. 112 (2002) 1405–1413.
[26] K. Yasui, T. Tuziuti, J. Lee, T. Kozuka, A. Towata, Y. Iida, The range of ambient radius for an active bubble in sonoluminescence and sonochemical reactions, J. Chem. Phys. 128 (2008) 184705.
[27] M. Ashokkumar, M. Hodnett, B. Zeqiri, F. Grieser, G.J. Price, Acoustic emission spectra from 515 kHz cavitation in aqueous solutions containing surface-active solutes, J. Am. Chem. Soc. 129 (2007) 2250–2258.

[28] J. Lee, M. Ashokkuar, S. Kentish, F. Grieser, Determination of the size distribution of sonoluminescence bubbles in a pulsed acoustic field, J. Am. Chem. Soc. 127 (2005) 16810−16811.
[29] K. Yasui, T. Tuziuti, J. Lee, T. Kozuka, A. Towata, Y. Iida, Numerical simulations of acoustic cavitation noise with the temporal fluctuation in the number of bubbles, Ultrason. Sonochem. 17 (2010) 460−472.
[30] G.J. Price, M. Ashokkumar, M. Hodnett, B. Zequiri, F. Grieser, Acoustic emission from cavitating solutions: implicationds for the mechanism of sonochemical reactions, J. Phys. Chem. B 109 (2005) 17799−17801.
[31] S.I. Madanshetty, R.E. Apfel, Acoustic microcavitation: enhancement and applications, J. Acoust. Soc. Am. 90 (1991) 1508−1514.
[32] R. Arieli, A. Marmur, Decompression sickness bubbles: are gas micronuclei formed on a flat hydrophobic surface? Respir. Physiol. Neurobiol. 177 (2011) 19−23.
[33] P.S. Epstein, M.S. Plesset, On the stability of gas bubbles in liquid-gas solutions, J. Chem. Phys. 18 (1950) 1505−1509.
[34] H.S. Carslaw, Introduction to the Mathematical Theory of the Conduction of Heat in Solids, Macmillan, London, 1921. Dover Pub., New York, 1945, HardPress Pub., Miami (FL), 2013.
[35] A. Brotchie, F. Grieser, M. Ashokkumar, Effect of power and frequency on bubble-size distributions in acoustic cavitation, Phys. Rev. Lett. 102 (2009) 084302.
[36] V.S.J. Craig, Very small bubbles at surfaces-the nanobubble puzzle, Soft Matter 7 (2011) 40−48.
[37] M.G. Sirotyuk, Cavitation strength of water and its distribution of cavitation nuclei, Sov. Phys. Acoust. 11 (1966) 318−322.
[38] K. Yasui, Y. Iida, T. Tuziuti, T. Kozuka, A. Towata, Strongly interacting bubbles under an ultrasonic horn, Phys. Rev. E 77 (2008) 016609.
[39] L.A. Crum, Measurements of the growth of air bubbles by rectified diffusion, J. Acoust. Soc. Am. 68 (1980) 203−211.
[40] O. Louisnard, F. Gomez, Growth by rectified diffusion of strongly acoustically forced gas bubbles in nearly saturated liquids, Phys. Rev. E 67 (2003) 036610.
[41] R. Mettin, Bubble structures in acoustic cavitation, in: A.A. Doinikov (Ed.), Bubble and Particle Dynamics in Acoustic Fields: Modern Trends and Applications, Research Signpost, Trivandrum (India), 2005, pp. 1−36.
[42] R. Mettin, I. Akhatov, U. Parlitz, C.D. Ohl, W. Lauterborn, Bjerknes forces between small cavitation bubbles in a strong acoustic field, Phys. Rev. E 56 (1997) 2924−2931.
[43] T.J. Matula, S.M. Cordry, R.A. Roy, L.A. Crum, Bjerknes force and bubble levitation under single-bubble sonoluminescence conditions, J. Acoust. Soc. Am. 102 (1997) 1522−1527.
[44] C.D. Ohl, M. Arora, R. Dijkink, V. Janve, D. Lohse, Surface cleaning from laser-induced cavitation bubbles, Appl. Phys. Lett. 89 (2006) 074102.
[45] V. Minsier, J. De Wilde, J. Proost, Simulation of the effect of viscosity on jet penetration into a single cavitating bubble, J. Appl. Phys. 106 (2009) 084906.
[46] M.O. Lamminen, H.W. Walker, L.K. Weavers, Mechanisms and factors influencing the ultrasonic cleaning of particle-fouled ceramic membranes, J. Membrane Sci. 237 (2004) 213−223.
[47] J. Holzfuss, M. Rüggeberg, A. Billo, Shock wave emissions of a sonoluminescing bubble, Phys. Rev. Lett. 81 (1998) 5434−5437.
[48] R. Hickling, M.S. Plesset, Collapse and rebound of a spherical bubble in water, Phys. Fluids 7 (1964) 7−14.
[49] R.T. Beyer, Nonlinear Acoustics, Acoustical Society of America, New York, 1997.
[50] W.L. Nyborg, Acoustic streaming near a boundary, J. Acoust. Soc. Am. 30 (1958) 329−339.
[51] S.A. Elder, Cavitation microstreaming, J. Acoust. Soc. Am. 31 (1959) 54−64.
[52] A. Moussatov, C. Granger, B. Dubus, Cone-like bubble formation in ultrasonic cavitation field, Ultrason. Sonochem. 10 (2003) 191−195.
[53] H. Mitome, S. Hatanaka, T. Tuziuti, Observation of spatial nonuniformity in a sonochemical reaction field, in: W. Lauterborn, T. Kurz (Eds.), Nonlinear Acoustics at the Turn of the Millennium (Proc. ISNA 15), AIP Conf. Proc, 524, 2000, pp. 473−476.

[54] N. Bremond, M. Arora, S.M. Dammer, D. Lohse, Interaction of cavitation bubbles on a wall, Phys. Fluids 18 (2006) 121505.

[55] K. Yasui, A. Towata, T. Tuziuti, T. Kozuka, K. Kato, Effect of static pressure on acoustic energy radiated by cavitation bubbles in viscous liquids under ultrasound, J. Acoust. Soc. Am. 130 (2011) 3233–3242.